Continental Shelf Research 84 (2014) 169–187

Contents lists available at ScienceDirect

Continental Shelf Research

journal homepage: www.elsevier.com/locate/csr

Research papers

Time-series measurements of settling particulate matter in Alfonso Basin, La Paz Bay, southwestern Gulf of California

Norman Silverberg [a,*], Fernando Aguirre-Bahena [a], Alfonso Mucci [b]

[a] Centro Interdisciplinario de Ciencias Marinas, Instituto Politécnico Nacional, Ave. IPN, Playa Palo de Santa Rita, La Paz, BCS, Mexico
[b] GEOTOP and Department of Earth and Planetary Sciences, McGill University, Montreal, QC, Canada

ARTICLE INFO

Article history:
Received 25 March 2013
Received in revised form
28 April 2014
Accepted 3 May 2014
Available online 22 May 2014

Keywords:
Sediment trap
Organic matter
Carbonate
Biogenic silica
Lithogenic
Eolian

ABSTRACT

More than 200 sediment trap samples were collected at 310 or 360 m depth during 2002–2009 from the center of the 410 m-deep Alfonso Basin in La Paz Bay, an arid, subtropical embayment of the southern Gulf of California. Sample splits were analyzed for total mass flux (TMF), particulate organic carbon (POC), inorganic carbon ($CaCO_3$) and opal (biogenic silica BioSi). The lithogenic (Litho) and biogenic fluxes (Biogen), but especially the particulate organic matter (POM) and $CaCO_3$, fluxes are relatively high compared with those recorded in a number of other coastal basins at depths less than ~500 m. The average yearly Litho fluxes (mean of 133 ± 158 g m^{-2} yr^{-1}) are well correlated with the frequency of strong wind gusts and reflect the relative proximity of the mooring to shore and the importance of eolian transport. The sedimentation patterns are influenced by monsoonal shifts—cool temperatures and strong northerly winds in late fall and winter sustain a well-mixed deep surface layer and high lithogenic fluxes, whereas progressive heating and relatively weak southerlies in summer and fall lead to a shallower, more-stratified surface layer with lower nutrient levels, limited productivity and generally low particulate fluxes. There is considerable interannual variability in the size of the various fluxes. This is likely related to a number of regional and internal factors whose timing, intensity and interactions remain to be resolved.

Although there is an inverse relationship between SST and satellite-derived net primary production (NPP) estimates, no correlation was found between NPP and the POC, $CaCO_3$ and BioSi fluxes ($r^2 < 0.05$ and $p > 0.05$). Significant correlations ($p < 0.001$) do exist, however, between the POC flux and the total mineral flux as well as with the $CaCO_3$, Litho and BioSi fluxes ($r = 0.86$, 0.82, 0.79 and 0.69, respectively). As suggested by the ballast ratio hypothesis, the strength of these correlations follows the relative density of the individual ballast components. Among the ballast minerals, the Litho fraction correlates strongly with $CaCO_3$ ($r = 0.84$), both fluxes being important during the windy cool season. The lithogenic fraction accounts for almost half of the total mass flux and is clearly a significant ballasting agent in this continental margin basin.

1. Introduction

La Paz Bay is a pristine environment of great biodiversity and productivity that supports an abundant variety of megafauna, including at least 16 cetacean species of temperate, tropical, and subtropical affinities, a growing colony of California sea lions and is visited by whale sharks and spine-tail devil rays (Pardo et al., 2013; Kahru et al., 2004; Reyes-Salinas et al., 2003; Lluch-Cota and Teniza-Guillén, 2000; Rodriguez Castañeda, 2008). The bay was designated as part of the "Área de Protección de Flora y Fauna Islas del Golfo de California" by the government of Mexico in 1978, was recognized as a UNESCO World Heritage site in 2005 and since 2007 includes the Parque Nacional del Archipelago de Espiritu Santo.

Despite the importance of the ecotourism industry it attracts, very limited monitoring of the environmental conditions in the bay has been carried out. To supplement the short-term studies undertaken to date of the oceanographic conditions (e.g. Jiménez-Illescas et al., 1997; Salinas-Gonzáles et al., 2003; Obeso-Nieblas et al., 2004; Monreal-Gómez et al., 2001) and ecology of the bay (e.g. Martínez-López et al., 2001; Reyes-Salinas et al., 2003), a sediment trap was deployed to measure the flux and composition of sinking particles in the bay.

The deepest portion of Alfonso Basin, the structural depression that occupies most of the northern portion of La Paz Bay (Fig. 1),

* Corresponding author. Tel.: +52 612 124 1682.
E-mail address: 1942norman@gmail.com (N. Silverberg).

http://dx.doi.org/10.1016/j.csr.2014.05.005
0278-4343/

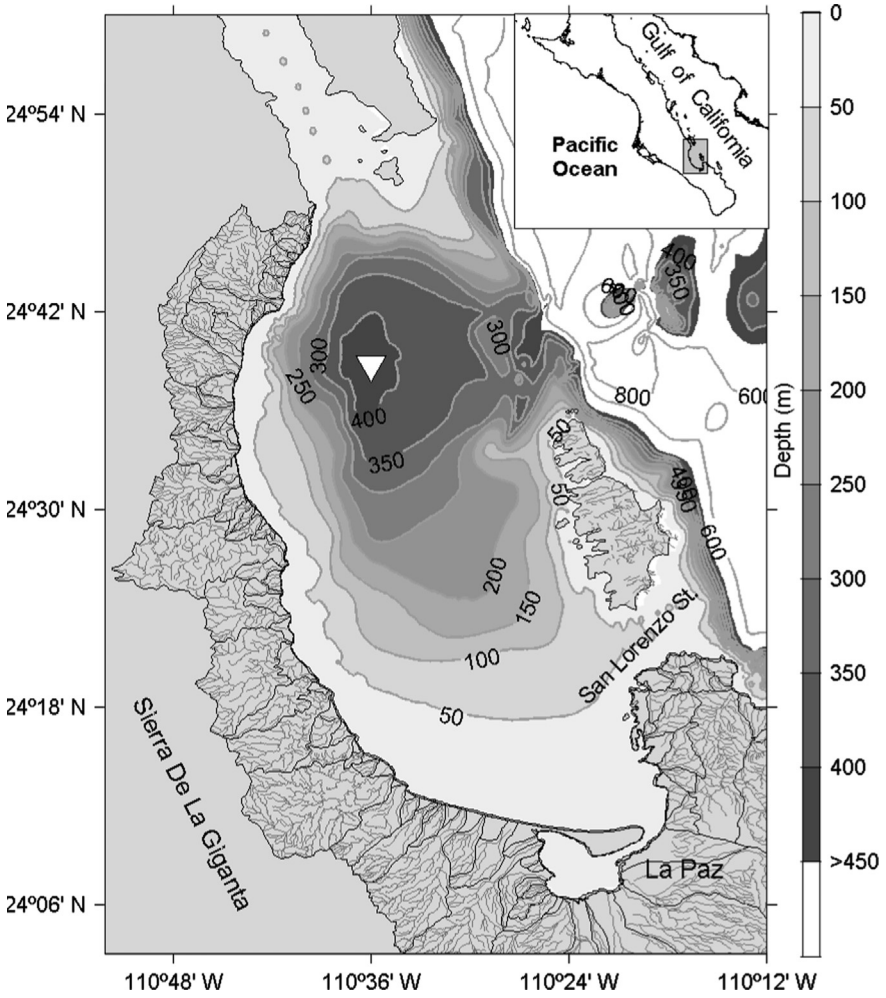

Fig. 1. Map showing the bathymetry of Bahîa de La Paz, its limited drainage basin and the location of the sediment trap mooring (white triangle).

was chosen as the site of the sediment trap mooring because: (a) it is a natural focus for sedimentation, (b) water movements are weak in the subsurface, (c) the dissolved oxygen concentration in the deep water is very low (<0.5–$1.0\ mL\ L^{-1}$) so that the occurrence of "swimmers" is limited, (d) the site is close to the land-based laboratories in La Paz and can be readily visited for periodic complimentary studies of the water column and servicing of the mooring, and (e) the data complements the time-series of sedimentation flux measurements carried out in Guaymas Basin between 1991 and 1997 in the central Gulf of California (Thunell, 1998).

Dugdale and Goering (1967) first formulated the concept of "new" primary production, further developed by Eppley and Peterson (1979), and that of the. "nutrient pump" (Emerson et al., 2001), representing the net flux of biologically produced organic matter from the surface to the interior of the oceans. Concerns about global warming led to research on how such "export' production, estimated with the aid of sediment trap data, might modulate the increase in atmospheric CO_2. A number of studies linked the variability in sediment trap fluxes to seasonal and interannual changes in hydrographic conditions and productivity in surface waters of the open ocean (e.g. Honjo et al., 1999; Thunell, 1997; Deuser et al., 1995; Deuser, 1986). Newer work (e.g. Karl et al., 1996; Lampitt and Anitia, 1997; Elskens et al., 2008), however, revealed an uncoupling between primary production and the flux of particulate organic carbon (POC) below the surface layer, indicating that other factors control the transfer of organic matter to deeper waters and the seafloor. Some of the ecosystem structure complexity affecting the transfer was discussed by Lutz et al. (2002, 2007). Consequently, although production in the surface ocean must provide for the biogenic particulate matter fluxes at depth, using sediment trap information to infer changes in the ecology of plankton in the photic zone is not straightforward.

Although it has long been known that the rate of organic carbon decay decreases as a power function with depth (e.g. Martin et al., 1987), Armstrong et al. (2002) showed that asymptotic models using the ratios of ballast particle fluxes to the POC flux lead to better predictions of organic carbon losses in the bathypelagic zone. "Ballast" particles are solid inorganic particles ($CaCO_3$ and opal biogenic tests, clay- or sand-sized particles) to which organic matter (OM) can be adsorbed and whose greater density augments the settling velocity of POM. Whereas POC: ballast flux ratios were found to be high and variable in the surface ocean, they converge to narrow ranges of values in the deep (below 1500–2000 m) ocean (Armstrong et al., 2002, 2009; Klaas and Archer, 2002). Thunell et al. (2007) showed that a similar convergence affects the POC flux at much shallower depths (200–1200 m) in the Cariaco Basin. In this context, the role of ballast components, particularly the lithogenic flux, in Alfonso Basin needs to be addressed.

The underlying scientific objectives of the present study were to examine processes related to export production and biogeochemical cycles in a subtropical, arid continental margin basin. To this end, the fluxes of the principal components of the settling particulate matter are examined over an 8-year period and compared with changes in satellite-derived estimates of sea surface temperature (SST) and primary productivity (PPN), wind

regime, and available information on the structure of the phytoplankon community.

1.1. Study area

The southern half of La Paz Bay consists of a broad, shallow, sand-covered shelf that narrows along the coast to the north and the islands forming the eastern margin of the bay. Bottom sediments become muddier as the shelf gradually deepens and then plunges to form the Alfonso Basin, which occupies most of the northern half of the bay (Cruz-Orozco et al., 1996; Nava-Sánchez, 1997). The drainage basin of La Paz Bay is restricted to a narrow band (6–17 km wide) between the Sierra de la Giganta mountains and the Gulf of California (Fig. 1). Lithogenic source material in the south of the bay consists mainly of granitic rocks and alluvium; andesitic volcanic and volcanoclastic rocks of the Comondo Formation form the bulk of the Sierra de La Gargantua to the north and west, while mostly clastic sedimentary rocks of the El Cien Formation are exposed in a small area of the west central margin of the bay (Hausback, 1984; Choumiline, 2011).

The climate (wind and rainfall data from the CIBNOR Comitán meteorological station on the southwest shore of La Paz Bay are available at http://intranet.cibnor.mx/meteo/ecibmet.html) is hot, semi-arid and influenced by monsoon-like seasonal winds (Fig. 2a). Northwesterly winds dominate in the winter and spring when rainfall is slight, whereas milder southerly winds occur in the late spring, summer and early fall (Badan-Dangon et al., 1991; Parés-Sierra et al., 2003; Marinone et al., 2004). During the latter period, intense heating of the surface layer induces strong stratification in the Gulf and pulses of land runoff occur with the advent of tropical storms (Monreal-Gómez et al., 2001; Obeso-Nieblas et al., 2004; Salinas-González et al., 2003). Except for hurricanes, measureable rainfall is limited to a few days each year (Fig. 2b).

The bay is influenced by regional atmospheric and oceanographic forcings, such as the North Pacific Gyre Oscillation (NPGO) and internal phenomena, such as isopycnal shoaling, intra-annual mesoscale gyres and the timing of shifts in wind direction and sea surface temperature (SST).

The water masses in La Paz Bay consist of Gulf of California Water (GCW), below which lies Subtropical Subsurface Water (StSsW) (Lavin and Marinone, 2003). Dissolved oxygen concentrations decrease rapidly below 50 m depth, with concentrations <1 mL L^{-1} by 100 m and <0.5 mL L^{-1} by 300 m (Monreal-Gómez et al., 2001). This reflects the free connection across the 275 m-deep sill at the northern mouth of the bay with the strong oxygen minimum in the subsurface water of adjacent southern Gulf of California (Alvarez-Borrego and Lara-Lara, 1991; Seibel, 2011). The very low O_2 concentrations below this depth suggest that the deepest water is not frequently replaced. Exchange through the much shallower San Lorenzo Strait at the southern mouth of the bay is limited to surface waters. The circulation pattern in the bay is still poorly documented but there is evidence, including drifter records, of a periodic cyclonic gyre centered over the deepest portion of the bay. This may be replaced episodically

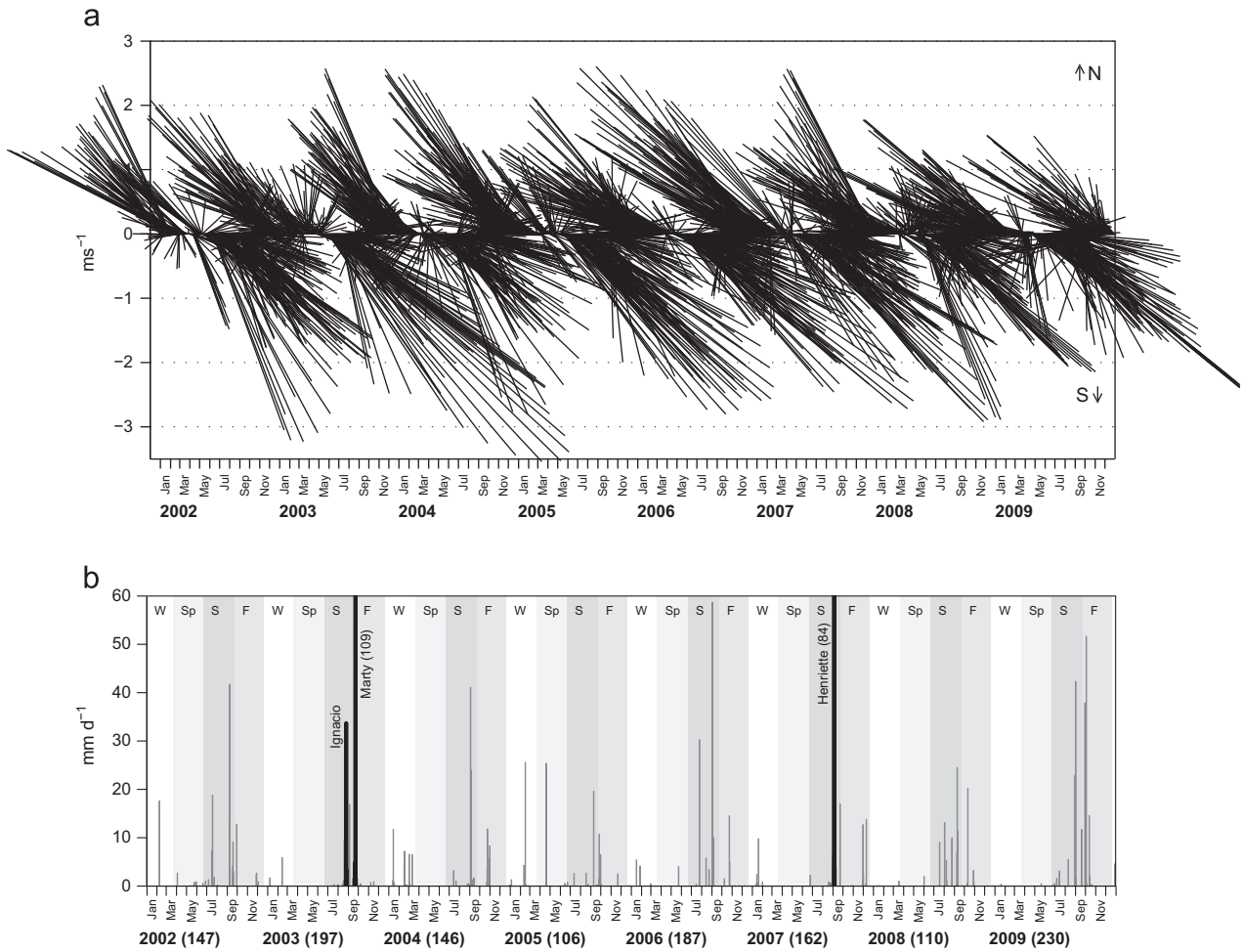

Fig. 2. Record of variations in (a) wind direction and intensity; (b) daily precipitation (mm) along with the total rainfall (in parentheses) for each year between 2002 and 2009.

by a roughly northern circulation or an anticyclonic gyre (Sánchez-Velasco et al., 2006; Monreal-Gómez et al., 2001; Villegas-Aguilera, 2009).

In winter, the southern Gulf of California is enriched in nutrients by upwelling along the eastern coast, associated with strong NW winds. The drift of these nutrient-rich waters towards the east contributes to the high primary production in the central Gulf. The deeper mixed layer in winter, as much as 90 m compared to as little as 10 m in summer (Villegas-Aguilera, 2009; Pardo et al., 2013), also sustains high Chl-a concentrations over much much of the southern Gulf during winter, whereas the summer months are characterized by low Chl-a, weaker southerly winds with little indication of upwelling along the western margin, and the intrusion of warm, oligotrophic Tropical Surface Water and Subsurface Subtropical Water into the southern Gulf (Alvarez-Borrego and Schwartzlose, 1979; Merrifield and Winant, 1989; Santamaría-del-Angel et al., 1994).

Limited direct primary productivity data exist for La Paz Bay. In general, primary production is high during winter and low during summer (Signoret and Santoyo, 1980; Reyes-Salinas et al., 2003; Cervantes-Duarte et al., 2005). Using a model integrating natural fluorescence, light penetration (1% of surface irradiance, critical depth between 40 and 80 m) and nutrient concentrations, Cervantes-Duarte et al. (2005) reported euphotic zone integrated primary production estimates ranging from 0.26 gC m^{-2} d^{-1} in November 2001 to 2.3 gC m^{-2} d^{-1} in June 2000. Likewise, using a similar modelling approach, Verdugo-Díaz et al. (2008) reported extremes in primary production of 0.55 gC m^{-2} h^{-1} for November 1997 and 0.76 gC m^{-2} h^{-1} for November 2000.

2. Methods

Settling particles were collected with a Technicap model PPS-3/3 sediment trap with a 0.125 m^2 (unbaffled) opening and a programmable, motor-driven carousel containing twelve 250-mL bottles. The instrument was installed close to 24°39′N, 110°36′W, 100 m above the seafloor at 310 m depth. Given navigational constraints in approaching the mooring position and lowering of the anchor weight, there may be as much as 5 m variation in the actual anchor depth. The height above the bottom was chosen to avoid possible contamination by resuspended material. Two suspended particulate matter concentration (0.1 to 1.4 mg L^{-1}) profiles obtained in 2002 from discrete depth samplings using 5-L Niskin bottles revealed no evidence of a deep nepheloid layer and, after learning that currents below the sill depth were very weak (Zaytzev et al., 2009), the trap was lowered to 50 m above the bottom (360 m depth) in November 2007. The mooring was anchored by 500 kg of cement blocks and supported by floats providing 160 kg of buoyancy. The mooring was serviced at 3 to 12-month intervals, providing, except for the technical glitches noted in the first paragraph of the Results section, continuous sampling with a 7 to 17-day resolution between 2002 and 2009.

The sample bottles contained a 4% formaldehyde solution of filtered (0.45 μm) seawater to which high purity NaCl was added to a practical salinity of 40, dense enough to limit exchange with the ambient seawater. Initially, the solution was pH-buffered using sodium phosphate, but some deterioration of foraminifera shells was noted in splits preserved for several months. The pH measured in these splits had decreased from 8.1 to 6.1–6.9. Therefore, beginning in August 2003, the buffer was changed to sodium tetraborate, which maintained a stable pH of about 8.

Once in the laboratory, a 1-mL aliquot of the recovered suspension was removed to a clean Petri dish and observed under a dissecting microscope equipped with a digital video recorder to document the general character of the material and identify the most conspicuous particles. After the aliquot was returned to the bulk sample, the latter was sieved through a 1000-μm Nylon screen to remove "swimmers" and large aggregates. This coarse fraction was stored in 20-mL vials for later examination. After sieving, the samples were subdivided into 10 equal subsamples ("splits") using a rotary splitter and transferred to 50-mL acid-washed plastic centrifuge tubes. Four of the tubes were pre-weighed, and these splits were centrifuged and the preservative solution decanted. The solid residue was rinsed with demineralized water to remove sea salts, centrifuged, decanted once again, and allowed to dry in a ~50 °C oven for at least 48 h. After cooling in a desiccator, the tubes were re-weighed and the split weight determined, (after 2007, the dried split was recovered from the tubes and weighed directly) from which the total mass flux (TMF) was estimated. The analytical error, determined from the standard deviation of the split weights, ranged from 0.001 to 0.213 g^{-2} d^{-1} and averaged 4.4% of the TMF.

2.1. Bulk biogenic component analyses

Initially, carbon analyses on splits and replicas from a total of 111 trap samples covering the period of 15 January, 2002 through 29 November, 2005 (Sample IDs I-1 through XI-2: See full Table 1 in Appendix A) were performed at the Laboratory of Ocean Chemistry, Shirsov Institute of Oceanology, Moscow, using the coulometric and dry combustion method of Ljutsarev (1987). Inorganic carbon (C_{inorg}) was determined as the difference between total carbon (C_{tot}) and organic carbon (C_{org}). Direct coulometric analyses of C_{inorg} on replicates of seven of our samples, (J. Murillo, personal com.), however, yielded absolute $CaCO_3$ concentrations that were on average 3% lower than those obtained by the difference method of Ljutsarev. For this reason, 84 previously analyzed samples (15 January 2002 through 29 November, 2005) for which there was still sufficient material available, as well as splits from 71 new samples (02 December, 2005 through 28 May, 2008, IDs XII-2 to XVIII-12) were analyzed coulometrically (UIC, Inc; Joliet, IL, USA) for C_{inorg} at the Department of Earth and Planetary Sciences, McGill University, following acidification with 2 N HCl and CO_2 extraction, using both pure $CaCO_3$ and Na_2CO_3 standard solutions for control. Replicate analyses yielded a relative precision of better than 3%. The total carbon (C_{tot}) and nitrogen (N_{tot}) content of splits of these same 155 samples was determined using the Carlo-Erba NC 2500 elemental analyzer at the GEOTOP facility of the Université du Québec à Montréal. The absolute instrumental reproducibility of these analyses, as determined from replicate measurements of Organic Analytical Standard substances (acetanilide, atropine, cyclohexanone-2,4-dinitrophenyl-hydrazone and urea), was estimated at $\pm$0.1% for C_{org} and $\pm$0.3% for N_{tot} and the relative analytical reproducibility was better than 2%. C_{org} was then determined by difference ($C_{org} = C_{tot} - C_{inorg}$). To complete the series, results of the 27 original samples (flagged by an * in Table 1) that were too small to be reanalyzed ($\ll$ 15 mg) were adjusted from the original Shirsov laboratory results, based upon the linear correlation ($r^2 = 0.863$) between all of the samples run at both the Moscow and Montreal laboratories. Between 29 May 2008 and 26 September 2009, 25 trap samples with sufficient mass for complete carbon analysis were recovered. Results for these samples, including replicates, were obtained from the laboratory of Dr. Juan Carlos Huergera, CICESE, Ensenada, using methods similar to those applied at McGill and GEOTOP. Relative analytical reproducibility was better than 3%. Analysis of a number of blind replicates successfully reproduced values for splits previously analyzed at McGill and GEOTOP. Finally, 6 samples of series XXII were analyzed for C_{org} at the Stable Isotope Facility, University of California at Davis and results are included in Table 1 to complete year 2009. Although the splits used for the analysis of

Table 1
Short: Summary results showing only the overall weighted means, raw standard deviations and the maximum and minimum values recorded.

	Total						Fluxes					
	Mass flux ($g\ m^{-2}\ d^{-1}$)	Corg (%)	N (%)	Corg:N (molar)	$CaCO_3$ (%)	BioSi (%)	Corg	$CaCO_3$	BioSi ($g\ m^{-2}\ d^{-1}$)	Biogen	Litho	Litho (%)
Overall Wtd. mean	0.675	8.08	1.12	9.0	12.1	26.2	0.049	0.087	0.173	0.388	0.342	42
St. dev'n (unWtd.)	0.663	2.45	0.43	1.1	4.3	14.6	0.029	0.086	0.154	0.280	0.433	12
Max	4.54	16.82	2.79	11.56	25.74	99.0	24.44	0.678	0.831	1.95	2.95	76
Min	0.043	1.03	0.14	0.35	2.58	6.03	0.001	0.004	0.009	0.050	0.011	6

inorganic carbon had been rinsed and dried soon after collection, because of the inadequate pH buffer used at the time, the results for samples taken between Jan 2002 and July 2003, are considered to be underestimates, and are flagged as such (*small italics*) in Table 1.

The biogenic silicon content (mole/g dry weight) was determined on a wet split using the sequential extraction method of DeMaster (1981). The weight fraction of biogenic silica (BioSi or opal) was then calculated by multiplying the silicon concentrations by a factor of 2.4, following Mortlock and Froelich (1989). The precision varied between 5 and 12%. The lithogenic fraction was estimated by subtracting the biogenic fraction (opal + particulate organic matter ([POM = 2.5 × C_{org}] following Thunell et al., 2007) + $CaCO_3$) from the TMF. Additional details about the analytical methodologies can be found in Aguirre-Bahena (2007).

3. Results

A compilation of the sediment trap sampling dates, as well as the computed total and major component fluxes are presented in Table 1 (See full table in Appendix A) and graphically according to year in Figs. 3 and 4. The yearly and overall means in Table 1 were calculated by weighting each parameter by the number of sampling days and dividing by the total number of days of collection. The weighted means minimize the effects of the variable sampling intervals dictated by the availability of shiptime to service the traps, the lack of sufficient material for certain analyses, and occasional failures in bottle rotation due to battery failure (e.g. 08 Jan–23 Feb 2003; 09 Jun–23 Sep 2004; 07 Nov 2006–17 Feb 2007) when all the material was collected in a single bottle. The corresponding standard deviations, however, refer to the raw data from each individual sample bottle.

Gaps in the record occurred on several occasions when the floating rope between the two GPS-positioned mooring-anchor weights was cut, apparently by fishing boats, and the instrument had to be recovered by pulling on a dragline run around the vertical portion of the mooring. These events (which fortunately have not recurred since 2006) led to delays in redeployment of the trap and, the loss of the last 5 bottles (04 Oct–13 Nov 2003), and, on one occasion (24 Feb–19 Sep 2006), the loss of an entire set of 12 samples. The zero values in the 2008 series were not due to any evident malfunction of the Technicap PPS3/3 instrument (which recorded the correctly sequenced programmed rotation of the carrousel), and appear to reflect periods of very limited sedimentation, as occurred in July 2002. Some material was recovered from these bottles, but not enough for analysis.

3.1. General composition of the settling particulate matter

Lithogenic material was often the most abundant component, making up between <1 and 76% of the mass of the samples, with an overall mean of 42% (Table 1). Its contribution, variably diluted by marine biogenic detritus, was commonly $>50\%$ between late fall and winter when northerly winds are strongest. Biogenic silica (fragments of diatoms, silicoflagellates and other siliceous microorganisms) was the most abundant biogenic component, accounting, on average, for 27% (range 6–99%) of the total mass. Its contribution was generally minimal in March, increased to a maximum in June and July when total mass fluxes were often minimal. The 99% value, for example, occurred in late June, 2002, when the TMF was only $0.065\ g^{-2}\ d^{-1}$ and consisted solely of numerous diatom chains. Values then decreased progressively through October, and increased again through late fall and early winter. $CaCO_3$ made up from 2.6 to 26% of the trap material, averaging 12.1%. There are very few sedimentary carbonate rocks among the mainly volcanic formations of the adjacent Baja Peninsula and factor analysis of the elemental composition of Alfonso Basin trap material indicates that the Ca is of biogenic origin (Rodriguez Castañeda, 2008; Choumiline, 2011), including fragments of foraminifera, coccoliths and other calcareous plankton. $CaCO_3$ concentrations were generally more abundant in late fall, whereas below average concentrations were typically recorded between May and July when the BioSi content was highest. Particulate organic matter (POM = 2.5 POC) made up between 2.6 and 42% of the weight of the sedimenting particulates. Averaging 20.3%, it was often more abundant than $CaCO_3$, particularly in spring and summer. Aguiñiga et al. (2010) reported that the $\delta^{13}C$ of Alfonso Basin trap material was between -19 and $-23‰$, close to that of marine phytoplankton (-18 to $-22‰$). The C_{org}:N_{tot} ratio of the trap samples for which data are available (Table 1) ranged between 5.7 and 11.6, with an overall mean of 8.9. The yearly means show a slight decrease between 2003 (10.0 ± 0.8) to 2007 (9.0 ± 0.4), whereas means of 7.7 ± 0.9 and 7.1 ± 0.5 were recorded for 2008 and 2009, respectively.

3.2. Particulate matter fluxes

3.2.1. Total mass, lithogenic and biogenic fraction fluxes

Dry weight total mass flux (TMF) determinations covering the period between January 18, 2002 and the end of 2009 were obtained from a total of 224 trap samples. The overall TMF weighted mean (Table 1) was $0.675\ g\ m^{-2}\ d^{-1}$.

^{234}Th disequilibrium measurements in the water column and of settling particulates, typically used to validate particle settling rates (Buesseler et al., 2007), were not available for this study. The overall mean TMF is equivalent to a sedimentation rate of $0.35\ mm\ yr^{-1}$, assuming an asymptotic water content of 50% by weight below 40–50 cm depth in the sediment. This compares well with independent, excess ^{210}Pb estimates of the accumulation rates from sediment cores recovered in the basin by Nava-Sánchez (1997), Pérez-Cruz (2000) and Rodriguez Castañeda (2008), of 0.5, 0.4 and $0.63\ mm\ yr^{-1}$, respectively; and $0.30\ mm\ yr^{-1}$ based upon ^{14}C dating (Pérez-Cruz, 2006). Hence, turbulence at the mouth of the trap did not appear to compromise the sediment trap capture efficiency in this environment of very weak deep currents (Zaytzev et al., 2009).

Our sediment trap data reveal temporal variations in the particulate flux, with total mass fluxes varying over two orders of magnitude (0.043 to $4.54\ g\ m^{-2}\ d^{-1}$), over the 8-year study

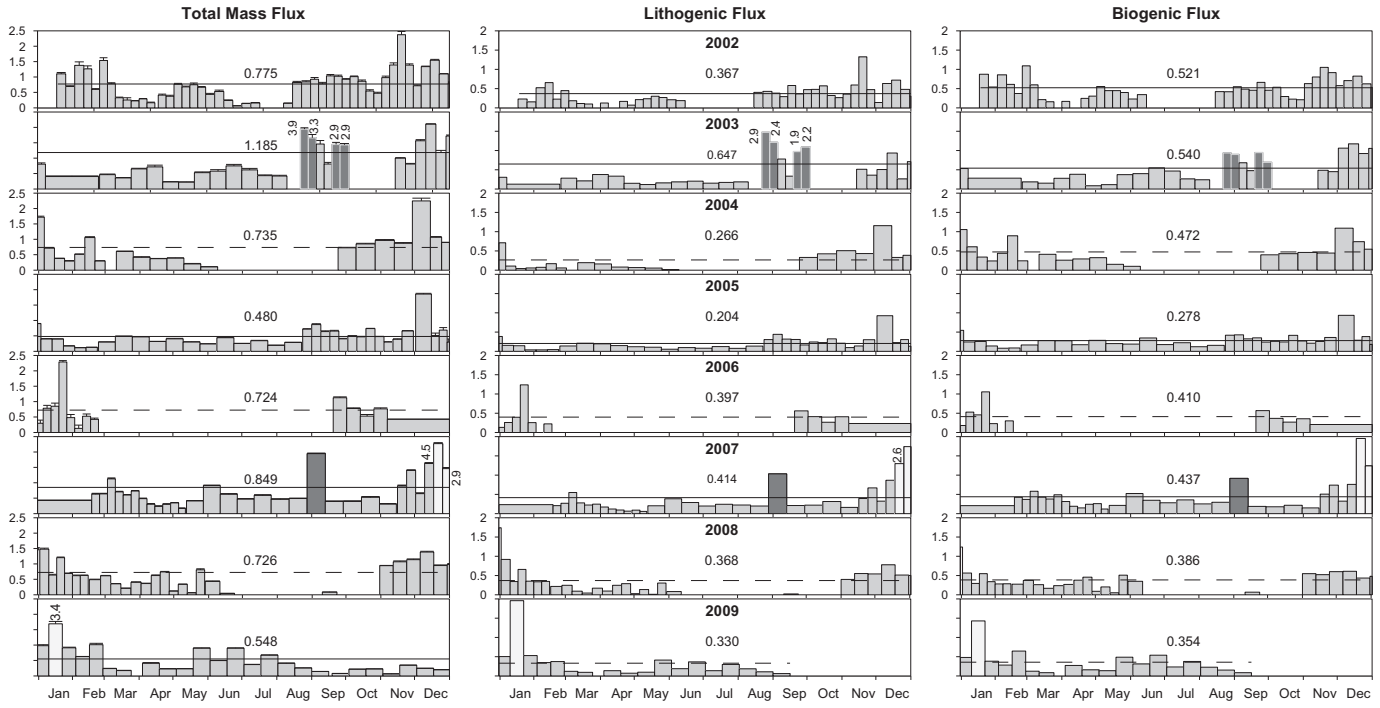

Fig. 3. The sediment trap record of the total mass, lithogenic and biogenic fluxes (g m^{-2} d^{-1}) between 2002 and 2009 in Alfonso Basin. Error bars shown for TMF represent the standard deviations of several splits from each trap. The number in the center and the horizontal lines (dashed when large gaps occurred) represent the raw annual mean. Black bars highlight the traps influenced by hurricanes Marty, Ignacio and Henriette, while white bars represent high fluxes associated with strong wind gusts, independent of hurricanes.

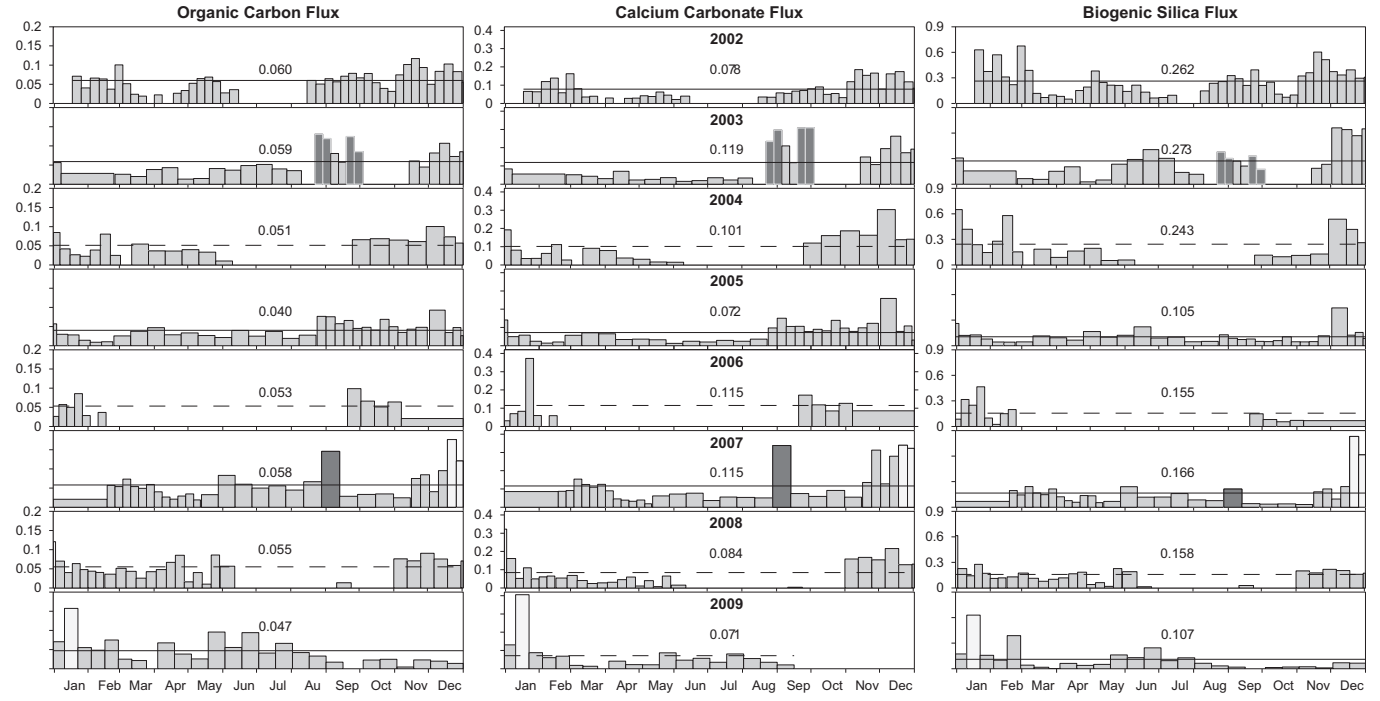

Fig. 4. The sediment trap record of the fluxes of biogenic silica (BioSi), calcium carbonate ($CaCO_3$), particulate organic matter (POM). The number in the center and the horizontal lines (dashed when large gaps occurred) represent the raw annual mean. Black bars highlight the traps influenced by hurricanes Marty, Ignacio and Henriette, while white bars represent high fluxes associated with strong wind gusts, independent of hurricanes. All units in g m^{-2} d^{-1}.

period. Likewise, the mean annual weighted TMFs display considerable year-to-year variability. The highest yearly-averaged TMF (0.91 g m^{-2} d^{-1} in 2003) can be partially accounted for by the four weekly samples recording the successive passage of hurricanes Marty and Ignacio (Silverberg et al., 2007). If these samples are excluded, the mean 2003 TMF drops to 0.69 g m^{-2} d^{-1}, very close to the overall mean of 0.68 g m^{-2} d^{-1}. The mean TMF in 2005 and 2009, (0.46 and 0.52 g m^{-2} d^{-1}, respectively) are substantially lower than those of all other sampled years.

A year-to-year comparison of the raw, unweighted, Total Mass, Lithogenic and Biogenic Fraction fluxes is presented graphically in Fig. 3. Higher than average fluxes frequently occurred during late

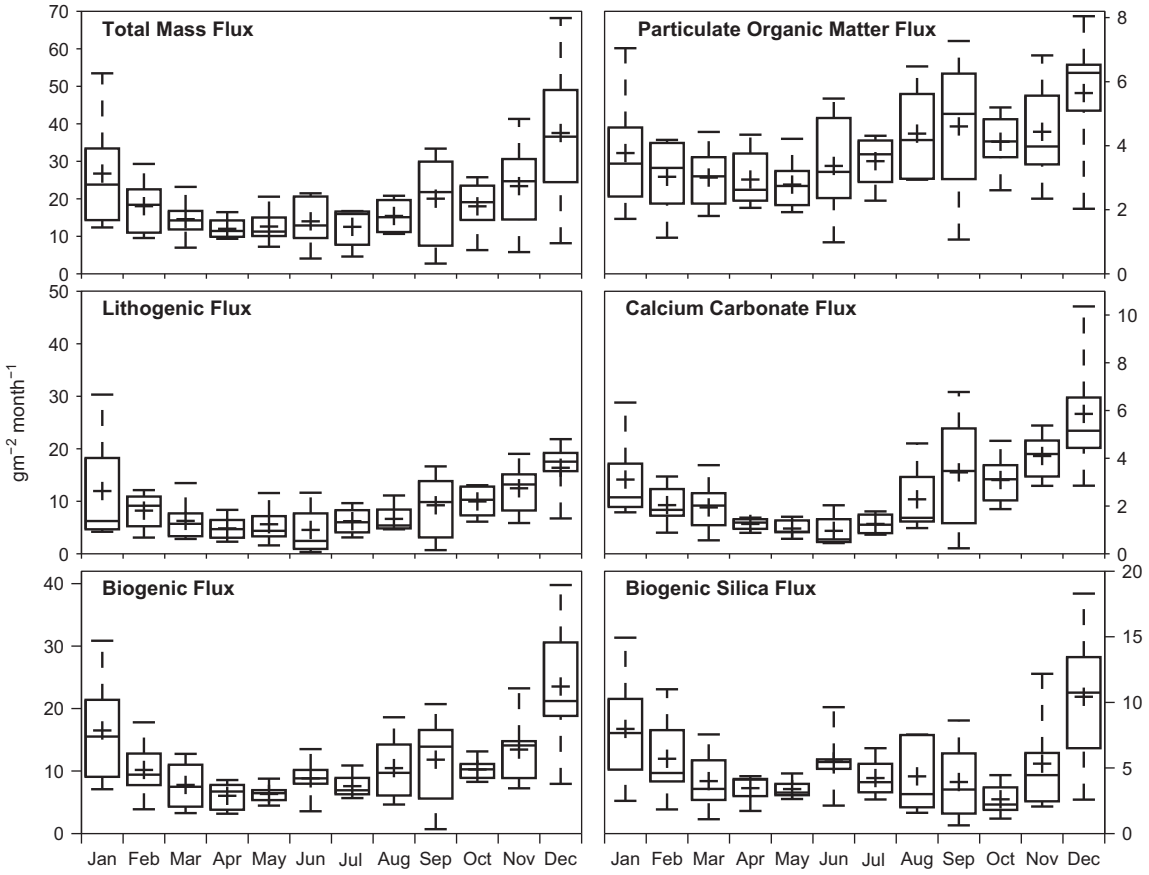

Fig. 5. Box and whisker diagrams showing the variation in the mean monthly fluxes of total mass, lithogenic and biogenic material, particulate organic matter, $CaCO_3$ and biogenic silica. +'s' represent the average, horizontal lines the median, the rectangular box encloses 25–75% of the data, while the "whiskers" enclose 9–91% of the data.

fall and early winter (November to February), and sometimes during August, September and October. Samples collected during and immediately following hurricanes (black bars in Fig. 3) recorded very high fluxes, but extreme fluxes (white bars in Fig. 3) also occurred during periods of high winds but no rain. Lower than average fluxes were typically recorded during spring and early summer. Nevertheless, the patterns are not consistent from year to year.

Similar patterns are observed among the biogenic components (Fig. 4). All show minimal yearly-averaged values for 2005 and 2009. Yearly-averaged BioSi fluxes were high from 2002 to 2004, but close to the overall mean (0.173 g m^{-2} d^{-1}, Table 1) from 2006 to 2008. The mean annual $CaCO_3$ fluxes oscillated between 0.07 and 0.11 g m^{-2} d^{-1}. The POC fluxes displayed relatively small changes, means between years ranging from 0.040 to 0.060 g m^{-2} d^{-1}.

3.2.2. *Mean monthly fluxes*

To better visualize the flux patterns over the year, the fluxes from the individual trap samples were recalculated on a monthly basis, using the cumulative mass that would have been intercepted by a single sample bottle from the beginning to the end of each month. This reduces the effect of occasional large sample-to-sample variations and samples that included overlapping months. When some days were unsampled, the value was extrapolated from the weighted daily mean and multiplied by the number of days in the month. No values were calculated for October 2003, because only the first 3 days were represented; the 1-day record for October 2008 was also not used.

Fig. 5 shows the resulting distribution of the weighted monthly fluxes between 2002 and 2009. The box and whiskers diagrams display a broad seasonality of the fluxes, with the lowest for each occurring during the spring and summer and the highest being observed in late fall and winter. The TMF also shows a secondary maximum in June, mostly accountable by BioSi and POM. There are some large spreads within the monthly fluxes, emphasizing the great interannual variability. The extreme spreads during August and September are mostly attributable to the passage of hurricanes Marty and Ignacio in 2003 whereas those of December are associated with a remarkable flux of both lithogenic and biogenic material at the end of that month in 2007.

4. Discussion

Despite a few large gaps in the sediment trap time-series, analyses of the samples recovered over the 8-year period provide valuable information about the nature and fluxes of settling particulate matter within Alfonso Basin. The data display much temporal variability, even on a weekly basis when such a resolution was available. Compared to Guaymas Basin, approximately 300 km to the north, seasonal patterns are less obvious and inconsistent between years. This probably reflects a greater variability in the physical environment of the southern Gulf of California, including occasional intrusions of warmer and less productive equatorial waters, northerly currents at the entrance to the Gulf (Lavin and Marinone, 2003) and the development of seasonal gyres in the southern Gulf that may affect La Paz Bay (Figueroa et al., 2003; Castro et al., 2006). Within the bay, there are periodic mesoscale gyres (Sánchez-Velasco et al., 2006), probably related to the shoaling of isopycnals (Villegas-Aguilera, 2009; Pardo et al., 2013). The ecological response within the upper water

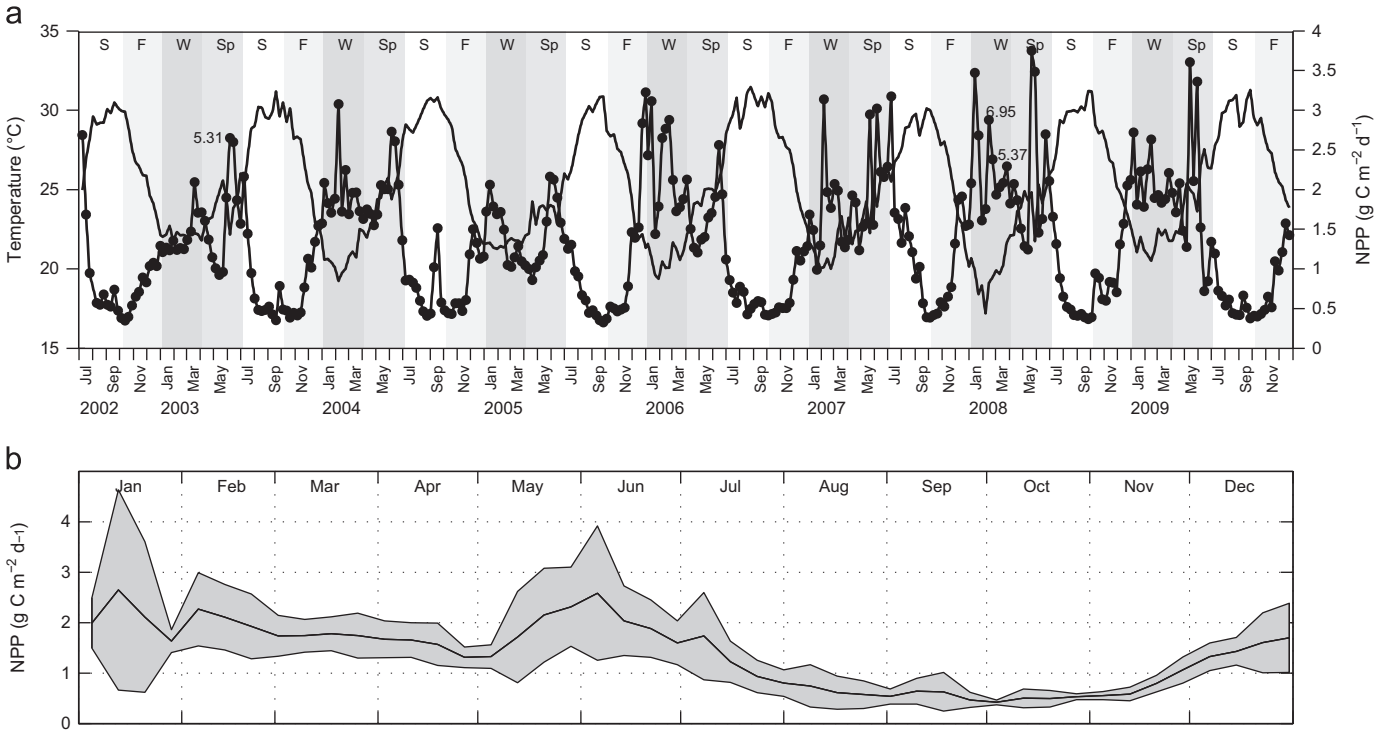

Fig. 6. (a) Record of 8-day satellite imagery derived data for the sea-surface temperature (SST, grey line) and the net primary production (NPP, black line with circles) for a 20×20 km grid, centered on Alfonso Basin. Note the association of higher NPP with low SST values. This relationship has a linear correlation (not shown) with $r = -0.77$. (b) Mean and range of the 8-day NPP data between 2002 and 2009.

column to such physical forcings, in turn, results in variations of plankton composition and the biologically-induced production of the aggregate particles that dominate the vertical flux (Silver and Gowing, 1991; Gonzalez et al., 2000; Roy et al., 2000). Martínez-López et al. (2012) reported that abundances of different silicoflagelate assemblages reflect alternations of subtropical, equatorial and subarctic influences and that the flux patterns show reasonable correlations with the Pacific decadal oscillation (PDO), North Pacific Gyre oscillation (NPGO), and El Niño Modoki indices. It remains to be seen if other ecosystem components, such as coccolithophores and foraminifera are affected by these broad variables within the southern Gulf of California.

The sediment trap time-series data reflect the influence of monsoonal shifts between northerly winds during the cool season in winter-spring and southerly winds during the hot season of summer-fall, but seasonal patterns in the sediment trap record are not predictable from year to year (Figs. 3 and 4). When the bulk sediment trap data are simplified by averaging monthly values for all years, the resulting box and whiskers diagrams (Fig. 5) highlight the low fluxes in summer compared to winter, but the spread of the data clearly reflects the large annual variability. The spread is influenced by episodic events, such as the irregular occurrence of secondary BioSi flux maxima in June, short-term phenomena, such as the impact of hurricanes Ignacio and Marty in Aug–Sep 2003, and the extraordinarily high flux of biogenic and lithogenic fluxes observed in December 2007.

4.1. Relationship of the fluxes to temperature and primary production

Unlike Guaymas Basin, where upwelling along the eastern margin of the Gulf of California during the northerly monsoon and strong temperature stratification in summer induce sharp seasonality in primary production as reflected in sediment trap records (Thunell, 1998), the southwestern margin of the Gulf is little influenced by upwelling, even during the southerly monsoon (Santamaría-del-Angel et al., 1994; Lluch-Cota et al., 2010). Nevertheless, as shown in Fig. 6a, there is significant seasonality in the satellite-derived net primary production (NPP) in La Paz Bay, higher productivity occurring mostly during periods of low SST. The data, using a 20×20 km grid centered on Alfonso Basin, are 8-day composites of Modis Aqua satellite Level 3, 4×4 km SST records available from http://oceancolor.gsfc.nasa.gov/cgi/l3, whereas the NPP estimates are derived from the standard Vertically Generalized Production Model (vgpm; Behrenfeld and Falkowski, 1997) algorithm, available at http://orca.science.oregonstate.edu/1080.by.2160.8day.hdf.vgpm.m.chl.m.sst4.php. Fig. 6b displays the mean and range of monthly NPP over the 8-year period. Note that the more productive months (between December and June, often with bimodal maxima) display greater interannual variability than those with low NPP (between July and November). Productivity is influenced by shifts in surface temperature, shoaling of the isopycnals and the depth of the surface mixed layer (Villegas-Aguilera, 2009; Pardo et al., 2013). There is some evidence that the shoaling phenomenon, accompanied by high Chl-α levels at the surface, is a yearly-recurrent intraseasonal event that sustains greater diatom productivity (Pardo et al., 2013).

The moderate seasonality in NPP does not correlate ($r^2 = 0.018$, $p = 0.25$) with the flux of POC (nor with that of BioSi or $CaCO_3$) recorded in the sediment trap during equivalent monthly collection periods (Fig. 7, left). The same is true of the SST (Fig. 7, right). Given that Chl-a concentrations typically display subsurface maxima and phytoplankton adapted to low-light contitions are abundant in Alfonso Basin (Villegas-Aguilera, 2009; Sidón-Ceseña, 2012), the integrated primary production derived from sea-surface satellite observations may not provide accurate estimates of the local productivity. The lack of coupling between production in the photic zone and POC export below the photic zone has been noted at a number of open ocean sites (Karl et al., 1996; Lampitt

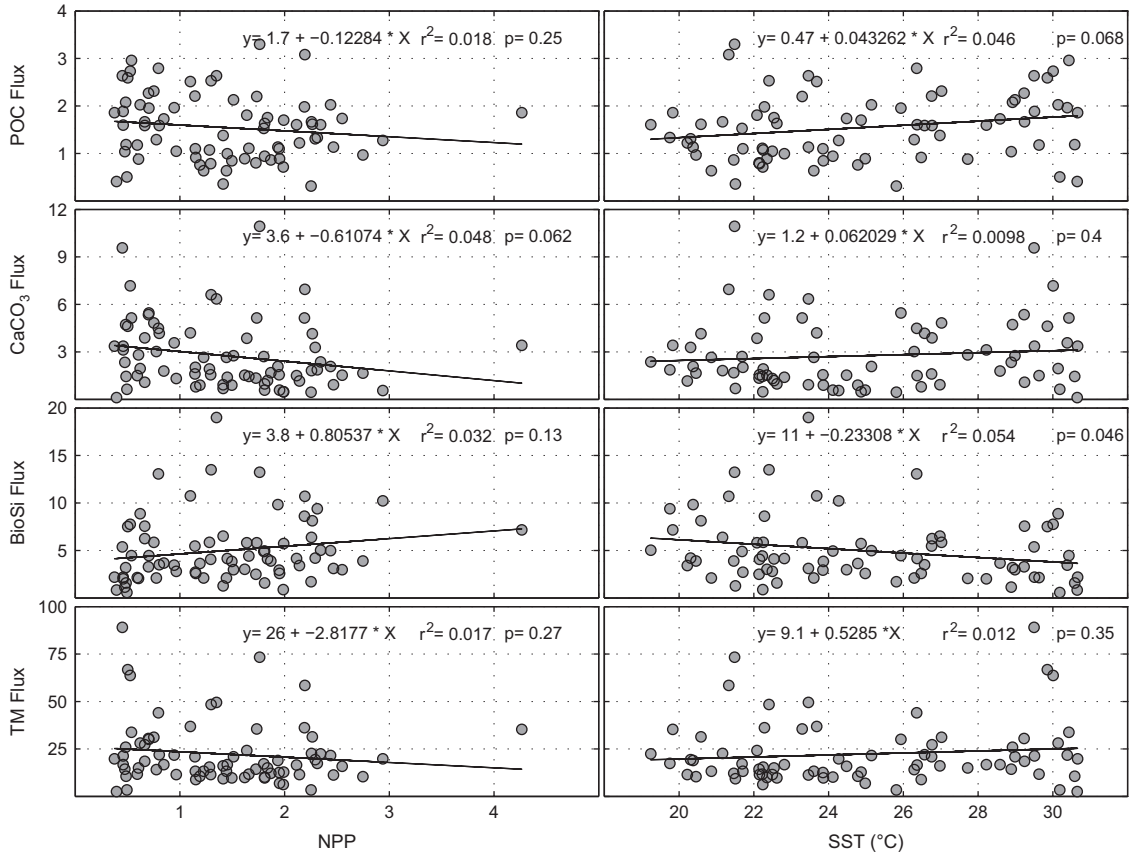

Fig. 7. (left) Linear regression fit of the satellite-derived mean monthly NPP versus the mean monthly POC, $CaCO_3$ and BioSi fluxes in corresponding sediment trap samples. (right). The same comparisons using SST. All units in g m^{-2} d^{-1}.

and Anitia, 1997; Elskens et al., 2008; Stukel et al., 2011). This implies a high degree of remineralization of fresh organic matter and dissolution of biominerals within the photic zone and in the underlying mesopelagic "twilight zone", as well as variable efficiency of "packaging" of organic matter into larger, rapidly settling aggregates, such as marine snow and fecal pellets (Silver and Gowing, 1991). Dunne et al. (2005) modeled the complex interaction between primary production, temperature, phytoplankton size structure and zooplankton grazing and POC export for a variety of open ocean provinces. They concluded that particle export is ultimately regulated by particle production and to a lesser degree by the ability to generate sinking material, the latter being dependent on phytoplankton size composition and temperature, with abundant large phytoplankton and relatively cold regions leading to more efficient POC export. Low POC export efficiencies in warm compared to cold environments have also been noted by Laws et al. (2000).

4.2. The relationship between ballast mineral and POC fluxes

In the open ocean, POC fluxes decrease exponentially with depth (e.g. Martin et al., 1987). Modelling of this phenomenon has led to the proposal that two classes of POC may exist: one consisting of free falling organic matter and the other associated with ballast particles, lithogenic mineral grains and the biominerals $CaCO_3$ and opal (Armstrong et al., 2002, 2009; Klaas and Archer, 2002; Lee et al., 2009). These studies showed that whereas POC:ballast ratios are high and variable in the surface ocean, they converge to a nearly constant value at depths >1800 m. Above this depth much of the POC is considered to be unprotected "unballasted" material with low settling velocity, and, thus efficiently remineralized (rapid exponential decay) in the upper water column. The greater density of the lithogenic and biogenic 'mineral' components increases the settling velocity of the aggregated organic matter. The latter is also thought to provide some form of mutual protection, i.e., reducing the rate of POC decay and mineral dissolution with depth. Accordingly, the "ballast ratio hypothesis" is that the fluxes of the ballast particles are good predictors of the POC flux in the bathypelagic zone of the open ocean (Armstrong et al., 2002, 2009; Klaas and Archer, 2002; Francois et al., 2002; Fischer et al., 2003).

The poor correlation between the POC flux at depth and primary productivity in the photic zone has also been noted in the Cariaco Basin on the continental margin of Venezuela (Thunell et al., 2007). Montes et al. (2012) showed that, for sediment traps located at 50 and 100 m depth within the photic zone of the Cariaco Basin, the POC flux was still significantly correlated with surface Chl-a, but that by 200 m depth, the biogenic fluxes had decreased by one order of magnitude and the correlation was lost. Furthermore, Thunell et al. (2007) also showed that the ballast flux was a good predictor of POC flux, not only for the multi-depth sediment trap arrays in Cariaco Basin, but also to the single-depth trap records for two other "upwelling-dominated" continental margin areas, Guaymas Basin in the central Gulf of California and Santa Barbara Basin off the California borderland.

Fig. 8a shows the linear regression correlations between the flux of various ballast components and POC for Alfonso Basin. The correlation coefficients obtained in Alfonso Basin, all significant with $p<0.001$, are very similar (Table 2) to those obtained for the three continental margin basins included in Thunell et al. (2007). Clearly, the ballast-ratio hypothesis, including the strong association with $CaCO_3$ (Klaas and Archer, 2002; Francois et al., 2002), accounts for much of the variability in the POC flux in continental

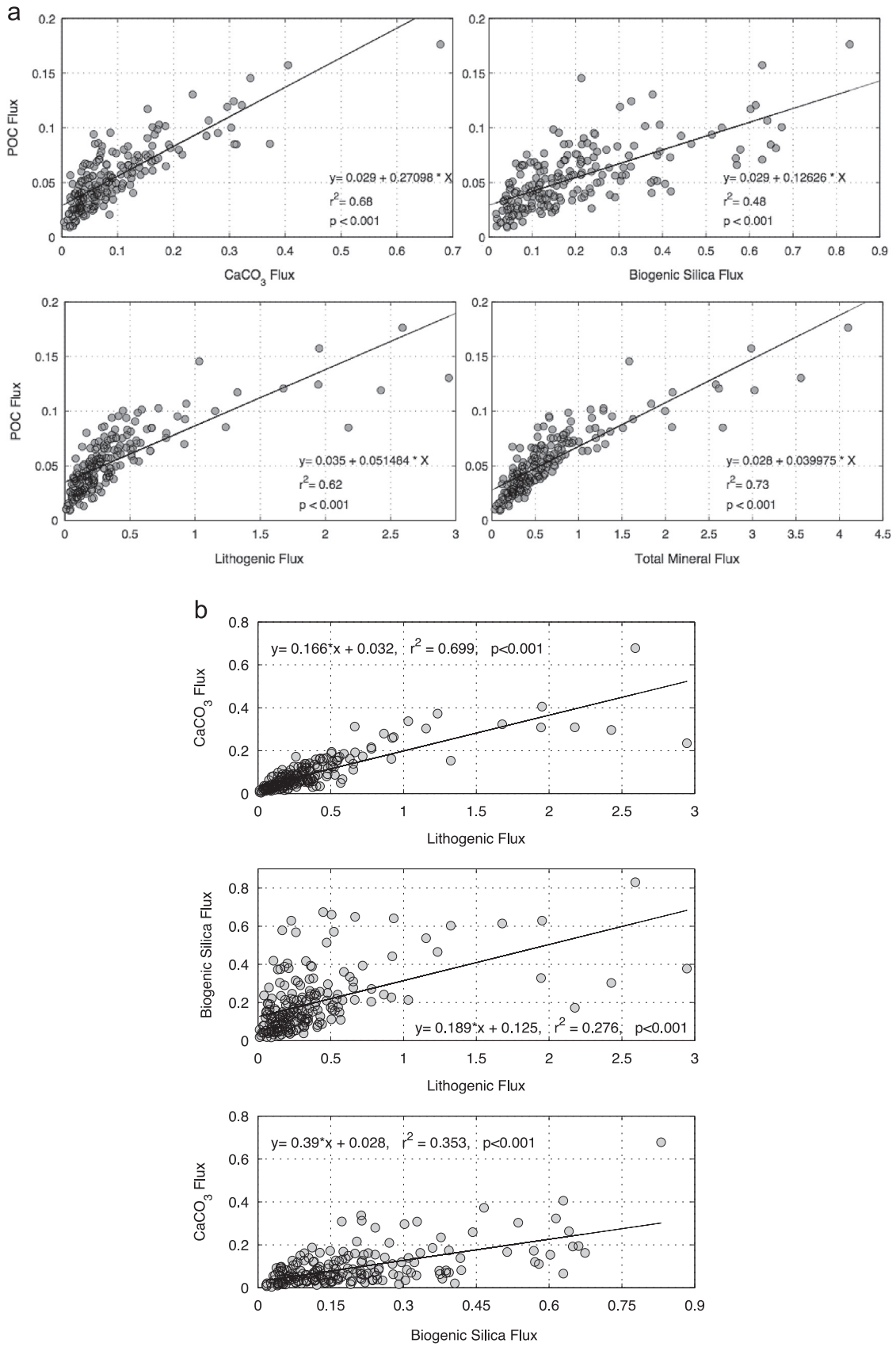

Fig. 8. (a) Linear least-squares regression between mean monthly fluxes of POC and total mineral ballast; lithogenic material, $CaCO_3$ and BioSi flux in sediment traps from Alfonso Basin. All units in g m^{-2} d^{-1}. (b) Linear least-squares regression between mean monthly fluxes of lithogenic, $CaCO_3$ and BioSi flux in sediment traps from Alfonso Basin. All units in g m^{-2} d^{-1}.

Table 2
Linear correlation coefficients between the POC flux versus that of and among the various ballast components in Alfonso Basin and the three seasonally-upwelling continental margin basins described in Thunell et al. (2007).

	Linear correlation coefficient r							
	POC vs. ballast minerals					Between minerals		
Basin	Trap depth	Total Mineral	$CaCO_3$	Lithogenic	BioSi	$CaCO_3$:Litho	$CaCO_3$:BioSi	BioSi:Litho
Alfonso	310, 360 (After Thunell et al., 2007 Table 2)	0.86	0.82	0.79	0.69	0.84	0.59	0.53
Guaymas	475	0.81	0.69	0.75	0.44			
Santa Barbara	500	0.81	0.84	0.69	0.78			
Cariaco	230	0.80	0.82	0.73	0.84			
	410	0.81	0.86	0.73	0.87			
	All depths	0.82	0.83	0.77	0.84			
All sites		0.79	0.84	0.65	0.75			

margin basins that are much shallower than the bathypelagic zone of the open ocean.

The correlation between the POC and BioSi fluxes in the various basins is highly variable (Table 2), which Thunell et al. (2007) ascribed to different diatom ecosystems. In Alfonso Basin, the BioSi:POC correlation coefficient is intermediate between that of Cariaco Basin, where "…diatoms dominate the phytoplankton during the winter-spring upwelling period…" and that of Guaymas Basin, where "…the late fall-early winter period of high opal fluxes is dominated by *Coscinodiscus* and *Rhizosolenia*, two genera with large cell volumes…". In Alfonso Basin, the siliceous phytoplankton assemblage is composed of varying abundances of relatively small-sized cells of *Chaetoceros*, *Pseudo-nitzchia*, *Pseudoguinardi* and *Dactyliosolen* diatoms and a lesser number of silicoflagellate cells such as *Octactis pulcra* (Villegas-Aguilera, 2009).

Among the ballast minerals themselves, (Fig. 8b) there is a strong correlation ($r=0.84$, $p<0.001$) between the $CaCO_3$ and Litho fluxes. Correlation coefficients are much lower for $CaCO_3$ vs. BioSi (0.59, $p<0.001$) and BioSi vs. Litho (0.53, $p<0.001$). Hence, the BioSi fluxes appear to be decoupled from the other ballast minerals. They are modulated by the nature and succession of diatom assemblages and their relative efficiency in transporting POC varies among marginal basins, possibly related to size structure (Thunell et al., 2007), and perhaps the manner by which BioSi becomes associated with POC (protection, adsorption, fecal pellets, marine snow). In Alfonso Basin, both lithogenic and $CaCO_3$ fluxes tend to be strongest during the fall and early winter (Fig. 5) as well as during strong hurricane events, coccolith production and fluxes apparently being stimulated by deep mixing of the water column at those times (Urcádiz-Cázares, 2005).

The two biominerals are generated during primary productivity (although $CaCO_3$ is also secreted by foraminifera and pteropods), so why should POC co-sediment preferentially with carbonate? Klaas and Archer (2002) attribute their relative transport efficiency to their relative density: calcium carbonate (2.71 g cm^3), lithogenic material (e.g. quartz 2.65 g cm^3), and opal (2.1 g cm^3). Furthermore, Engel et al. (2009b) suggested that biogenic calcite helps in the preservation of particulate organic matter (POM) by offering structural support for organic molecules. Nevertheless, other laboratory investigations of the association of POC with aggregate material (e.g. Iversen and Ploug, 2010; De La Rocha et al., 2008; Engel et al., 2009a) permit a variety of interpretations, and much of the work on marine snow aggregate formation and sinking (Alldredge and Silver, 1988; Passow et al., 2001) indicates that POM production and the aggregation phenomena modulate the mineral flux, rather than the opposite (Passow, 2004; Passow and De La Rocha, 2006). Trull et al. (2008) shared this opinion but suggested that whereas POM may control mineral fluxes in the upper ocean, the process grades to mineral control of the POM flux at depth. Continental margins are typically richer in both organic matter production and particle-aggregating organisms and receive much greater input of terrigenous minerals than the open ocean. More information on the mechanisms that govern POM degradation processes and mineral dissolution in the twilight zone are needed to better understand the role of such environments in global geochemical cycles.

4.3. The importance of the lithogenic flux in Alfonso Basin

On average, the lithogenic fraction accounts for almost half of the TMF in Alfonso Basin, and clearly plays an important role in the transfer of POC to the deep water and sediments of this continental margin basin. Since Fe does not limit primary production close to the continent, primary productivity is independent of lithogenic material input in Alfonso Basin, although mechanisms (wind stress) that bring lithogenic components to Alfonso Basin may promote productivity by increasing the surface mixed layer depth. In contrast, one cannot readily dissociate the $CaCO_3$ and BioSi fluxes from primary productivity since they may be produced by the same organisms. With the exception of the very high fluxes associated with the infrequent passage of hurricanes over the narrow local drainage basin, lithogenic material is likely exported to the bay by eolian transport. Ternon et al. (2010) showed that in the Ligurian Sea the strongest POC fluxes were concomitant with large increases of the lithogenic marine flux, which had originated from recent and stored Saharan dust fallout events, as well as some riverine input. Rain gauges are few and far between in Baja California Sur and while the records from CIBNOR may not properly reflect precipitation further north along the bay, there is little correlation between the measured rainfall (Fig. 2b) and lithogenic fluxes.

The wind rose diagram (Fig. 9a) shows that the wind direction azimuths are constrained, particularly those associated with gusts strong enough to initiate erosion during the northern and southern monsoons. To evaluate the impact of wind transport, we calculated the number of wind gusts >4.5 m s^{-1} at 9 m height, the approximate threshold velocity for erosion of fine-sand modal desert soil (Helm and Breed, 1999; following Bagnold, 1941). The number of wind gusts was then summed over each year, excluding times influenced by hurricanes Ignacio, Marty and Henrietta. Although there is a significant correlation ($r=0.74$, $p=0.035$) between the total number of strong gusts in each year and the mean annual lithogenic flux to the sediment traps, most of this can be ascribed to northerly (WNW-N) gusts ($r=0.82$, Fig. 9b) rather than those from the south ($r=0.25$, pâ^{a}¢0.05). This suggests that most of the windblown material originates from the coastal alluvium and the volcanic mountains to the N-WNW, rather than the alluvial deposits of the coastal plain and the granitic massif to the south of the bay, and even less to the fluvial drainage basin to

the west. Over the period of investigation, the number of intense wind gusts was lowest in 2005, as were both the lithogenic and biogenic fluxes. Periods of strong wind gusts, without rainfall, occurred just prior to the extreme TMFs of December 2007 and January 2009.

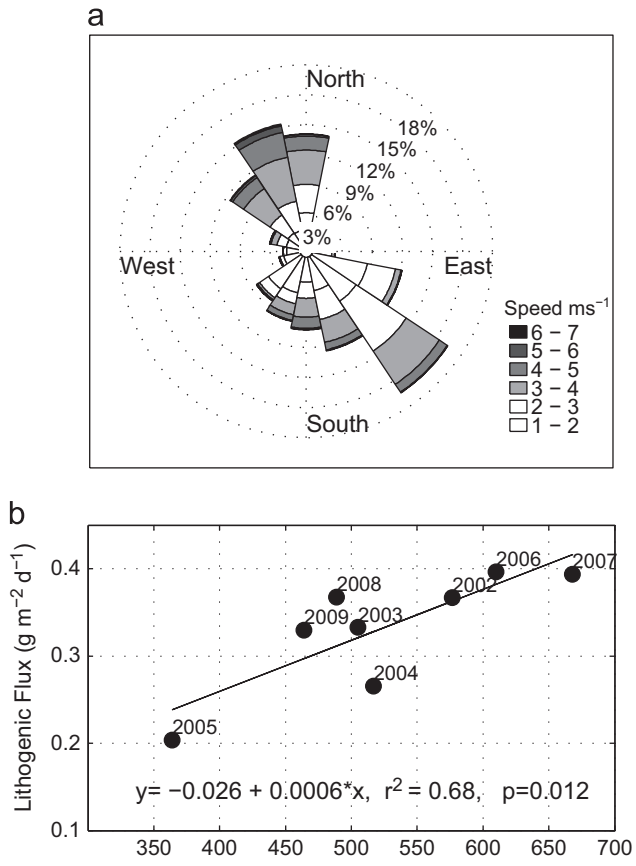

Fig. 9. (a) Windrose diagram showing the frequency (concentric rings), intensity and direction of winds recorded every 30 min between 2002 and 2009 at the CIBNOR meteorological station, La Paz Bay. (b) Linear least-squares regression (exclusive of hurricanes) between the annual mean lithogenic flux and the total number of wind gusts >4.5 m s^{-1} with the azimuth constrained to WNW-N, to include the greatest frequency of strong winds from the north (a).

4.4. Comparisons with other marginal basins

Table 3 shows that marginal basins can exhibit large differences in the fluxes and composition of the settling particulate matter. Despite the very limited land runoff, lithogenic matter fluxes account for almost half of the relatively high total mass flux in Alfonso Basin. They are almost three times greater than the mainly eolian input measured in Guaymas Basin (Thunell, 1998), but the Guaymas Basin trap was moored about 55 km from the Sonora coastline, whereas our trap sat only 12 km from shore. The biogenic component fluxes in Alfonso Basin are greater or equal to those in the basins listed in Table 3, except for the Santa Barbara Basin. Particulate fluxes in the Santa Barbara Basin display very strong seasonality, with high primary production in the spring and early summer and high river runoff in the fall and winter, enough to form annual varves in the underlying anoxic sediments. Despite the inverse seasonal relationship between the Litho and POC fluxes, the latter are sufficient even during the winter to yield a very high mean annual POM flux in Santa Barbara Basin. Because the various trap depths from the sites listed in Table 3 lie within the twilight zone of exponential POC flux decay, direct comparisons may be somewhat misleading. To better compare the export production in these coastal basins, values for the POC fluxes extrapolated to a common (photic zone) depth of 100 m are included in Table 3. The extrapolations were carried out according to the Martin POC-flux decay curve (Martin et al., 1987) that Montes et al. (2012) believe applicable to the POC fluxes in Cariaco Basin. Despite the lack of strong seasonal upwelling, the mean POC flux out of the photic zone in Alfonso Basin, 53 g m^{-2} yr^{-1}, is similar to the Cariaco Basin and is larger than in the Guaymas Basin and several other marginal basins. In order to maintain such a large mean POC flux, despite the lack of the marked seasonality that commonly occurs in cooler climates and seasonal wind-generated upwelling areas, requires sustained moderate productivity throughout the year.

5. Conclusions

Fluxes of both lithogenic and biogenic components of settling particulate matter in Alfonso Basin are moderately high compared to other continental margin basins. The seasonally-alternating northerly and southerly wind regime influences the sedimentation pattern with fluxes, on average, being highest during the late fall and winter and

Table 3
Mean annual total mass and other sediment trap component fluxes in a number of continental margin basins. The POC flux, extrapolated to the base of the photic zone (100 m) using the Martin curve (Martin et al., 1987) is included to aid comparison of organic carbon export.

Mean annual Flux (g m^{-2} y^{-1})	Hidaka Basin (520 m)[a] Japan Margin	Laurentian trough (150 m)[b] Gulf of St. Lawrence	Cariaco Basin (230 m)[c] Caribbean Sea	Santa Barbara Basin (500 m)[c] California Margin	San Lazaro Basin (330 m)[d] Baja Margin	Gulf of Tehuantepec (350 m)[e] Southern Mexican Pacific	Guaymas Basin (475 m)[c] Gulf of California	Alfonso Basin (310;350 m)[f] Gulf of California
Total mass	105	174	327	818	89	107	152	269
Lithogenic	43	134*	187	529			52	133
BioSi	29	–	32	135			63	67
$CaCO_3$	12	5	42	66		10	18	34
POM	8	35	68	88	19	18	19	44
POC @ 100 m	22	20	55	139	21	21	29	53

After.

* Litho + BioSi.
[a] Otosaka and Noriki (2005).
[b] Silverberg et al. (2000).
[c] Thunell et al. (2007).
[d] Silverberg et al. (2004).
[e] Machain-Castillo et al. (2009).
[f] This study.

lowest in summer, but there is much variability from year to year. Extreme fluxes are associated with hurricanes that impact the area in some years during late summer, whereas others follow periods of strong gusts but no rainfall. The exact causes of the interannual variability remain unknown, but are probably the result of interactions of both local and regional forcings.

Primary production estimates derived from satellite imagery are poor predictors of the fluxes of the biogenic components, POC, $CaCO_3$ and BioSi, below the photic zone. As in other continental margin basins, the fluxes of $CaCO_3$, lithogenic material and BioSi, in that order (save for the Cariaco Basin, where BioSi is the dominant ballast mineral), correlate with the POC flux. Among these ballast components, there is significant correlation between the lithogenic and $CaCO_3$ fluxes, but both are more poorly correlated with the BioSi flux. The sedimenting lithogenic material appears to be of eolian origin, the source being mostly constrained to the N-WNW during winter, when winds are strongest. It makes up almost half of the total mass flux and is clearly an important ballasting agent in Alfonso Basin. Lithogenic fluxes may perhaps be more useful paleoceanographic indicators of POC sedimentation han the more labile biogenic fluxes, particularly in areas close to the continents.

Acknowledgements

We would like to thank the officers and crew of the B.O."Francisco de Ulloa" for their professional assistance in deploying and recovering the sediment trap mooring, as well as the various students and professors who assisted on many cruises. This research was supported by grants from the Instituto Politécnico Nacional of Mexico (SIP "Monitoreo Ecológico Continuo en Bahía de La Paz: Serie de Tiempo" 20060199, 20070664, 20080650, 20090523) and from the Consejo Nacional de Ciencia y Tecnología of Mexico (CONACyT 47310 Variaciones estacionales e interanuales en los flujos y la composición de materia particulada en hundimiento en la Bahía de La Paz y los factores biológicos y físicos que lo controlan).

Appendix A

Table 1
Results of the analyses of sediment trap samples collected between 2002 and 2009 in Alfonso Basin, SW Gulf of California.

			Total						Fluxes					
Sample	Sample	No.	Mass Flux	Corg	N	Corg:N	$CaCO_3$	BioSi	Corg	$CaCO_3$	BioSi	Biogen	Litho	Litho
Dates	ID	Days	g/m^2/d	%	%	(molar)	%	%	g/m^2/d					%
2002														
1–17 Jan		17	nd	nd	nd	nd	nd	nd	nd	nd	nd	nd	nd	
18–25 Jan [a]	I-1	8	1.102	6.44	0.69	10.8	*6.00*	57.1	0.071	*0.066*	0.629	*0.873*	*0.229*	*21*
26 Jan–2 Feb	I-2	8	0.692	5.83	0.66	10.3	*9.17*	54.1	0.040	*0.063*	0.375	*0.539*	*0.153*	*22*
3–10 Feb	I-3	8	1.378	4.79	nd	nd	*8.68*	41.4	0.066	*0.120*	0.571	*0.856*	*0.522*	*38*
11–17 Feb	I-4	7	1.263	5.04	0.61	9.7	*11.0*	24.6	0.064	*0.139*	0.310	*0.608*	*0.655*	*52*
18–24 Feb	I-5	7	0.597	6.20	0.79	9.2	*9.74*	36.8	0.037	*0.058*	0.220	*0.370*	*0.227*	*38*
25 Feb-3 Mar	I-6	7	1.535	6.55	0.81	9.4	*10.6*	43.9	0.101	*0.162*	0.674	*1.088*	*0.447*	*29*
3–10 Mar	I-7	7	0.780	6.58	0.79	9.7	*10.3*	49.7	0.051	*0.081*	0.388	*0.597*	*0.183*	*23*
11–17 Mar [a]	I-8	7	0.326	7.31	nd	nd	*10.8*	36.1	0.024	*0.035*	0.118	*0.213*	*0.114*	*35*
18–24 Mar [a]	I-9	7	0.255	7.51	nd	nd	*15.4*	27.2	0.019	*0.039*	0.069	*0.156*	*0.098*	*39*
25–31 Mar	I-10	7	0.227	nd	nd	nd	nd	43.6	nd	nd	nd	nd	nd	
1–7 Apr [a]	I-11	7	0.291	7.63	nd	nd	*10.2*	28.3	0.022	*0.030*	0.082	*0.168*	*0.124*	*42*
7–14 Apr	I-12	7	0.166	nd	nd	nd	nd	30.0	nd	nd	nd	nd	nd	
15–17 Apr		3	nd	nd	nd	nd	nd	nd	nd	nd	nd	nd	nd	
18–24 Apr [a]	II-1	7	0.413	6.41	nd	nd	*6.63*	36.5	0.026	*0.027*	0.151	*0.244*	*0.169*	*41*
25 Apr-1 May [a]	II-2	7	0.374	9.00	nd	nd	*7.76*	51.2	0.034	*0.029*	0.192	*0.305*	*0.070*	*19*
2–8 May [a]	II-3	7	0.764	6.85	nd	nd	*5.46*	49.8	0.052	*0.042*	0.380	*0.553*	*0.211*	*28*
9–15 May	II-4	7	0.682	9.52	1.16	9.6	*5.58*	36.1	0.065	*0.038*	0.246	*0.447*	*0.235*	*34*
16–22 May	II-5	7	0.747	9.21	1.21	8.9	*8.35*	28.6	0.069	*0.062*	0.214	*0.448*	*0.299*	*40*
23–29 May	II-6	7	0.667	8.52	1.01	9.8	*6.75*	31.7	0.057	*0.045*	0.211	*0.398*	*0.268*	*40*
30 May–6 Jun [a]	II-7	8	0.438	6.23	nd	nd	*4.84*	32.0	0.027	*0.021*	0.140	*0.230*	*0.208*	*48*
7–14 Jun [a]	II-8	8	0.529	6.77	nd	nd	*7.48*	40.4	0.036	*0.040*	0.214	*0.343*	*0.186*	*35*
15–22 Jun	II-9	8	0.236	nd	nd	nd	nd	55.8	nd	nd	nd	nd	nd	
23–30 Jun	II-10	8	0.065	nd	nd	nd	nd	99.0	nd	nd	nd	nd	nd	
1–8 Jul	II-11	8	0.138	nd	nd	nd	nd	50.5	nd	nd	nd	nd	nd	
9–16 Jul	II-12	8	0.157	nd	nd	nd	nd	61.1	nd	nd	nd	nd	nd	
17 Jul–6 Aug		21	nd	nd	nd	nd	nd	nd	nd	nd	nd	nd	nd	
7–14 Aug	III-1	8	0.149	nd	nd	nd	nd	99.0	nd	nd	nd	nd	nd	
15–22 Aug	III-2	8	0.823	7.27	0.81	10.4	*4.25*	28.7	0.060	*0.035*	0.236	*0.421*	*0.402*	*49*
23–30 Aug	III-3	8	0.843	5.98	0.68	10.3	*4.00*	30.5	0.050	*0.034*	0.257	*0.417*	*0.427*	*51*
31 Aug–6 Sep	III-4	7	0.926	6.97	0.76	10.7	*6.25*	35.3	0.065	*0.058*	0.327	*0.546*	*0.380*	*41*
7–13 Sep	III-5	7	0.777	7.24	0.90	8.9	*7.10*	37.4	0.056	*0.055*	0.290	*0.486*	*0.291*	*37*
14–20 Sep	III-6	7	1.038	6.84	0.74	10.7	*6.50*	20.4	0.071	*0.067*	0.212	*0.457*	*0.581*	*56*
21–27 Sep [a]	III-7	7	1.023	7.66	nd	nd	*6.92*	38.5	0.078	*0.071*	0.394	*0.660*	*0.363*	*35*

28 Sep–4 Oct	III-8	7	0.929	7.19	0.88	9.6	*8.59*	22.6	0.067	*0.080*	0.211	*0.457*	*0.472*	*51*
5–11 Oct	III-9	7	1.014	7.71	0.94	9.5	*8.93*	24.6	0.078	*0.091*	0.249	*0.535*	*0.478*	*47*
12–18 Oct	III-10	7	0.863	6.27	0.68	10.8	*5.75*	12.6	0.054	*0.050*	0.109	*0.294*	*0.569*	*66*
19–25 Oct [a]	III-11	7	0.544	7.17	nd	nd	*10.0*	13.4	0.039	*0.054*	0.073	*0.225*	*0.319*	*59*
26 Oct – 01 Nov [a]	III-12	7	0.474	6.58	nd	nd	*6.68*	20.9	0.031	*0.032*	0.099	*0.209*	*0.265*	*56*
2–8 Nov	IV-1	7	0.982	7.59	0.85	10.5	*12.1*	32.8	0.075	*0.119*	0.322	*0.628*	*0.355*	*36*
9–15 Nov	IV-2	7	1.390	7.30	0.82	10.4	*13.3*	25.9	0.101	*0.185*	0.360	*0.799*	*0.591*	*43*
16–22 Nov [a]	IV-3	7	2.374	4.94	nd	nd	*6.47*	25.4	0.117	*0.154*	0.602	*1.049*	*1.325*	*56*
23–29 Nov	IV-4	7	1.386	6.77	0.82	9.6	*12.0*	37.1	0.094	*0.166*	0.514	*0.914*	*0.471*	*34*
30 Nov–6 Dec	IV-5	7	0.715	6.99	0.78	10.4	*11.1*	52.3	0.050	*0.079*	0.373	*0.577*	*0.137*	*19*
7–14 Dec	IV-6	8	1.336	6.25	0.80	9.2	*12.1*	25.0	0.084	*0.162*	0.334	*0.705*	*0.631*	*47*
15–22 Dec	IV-7	8	1.543	6.65	0.88	8.8	*11.3*	25.5	0.103	*0.174*	0.394	*0.825*	*0.718*	*47*
23–30 Dec	IV-8	8	1.102	7.53	0.94	9.3	*10.7*	26.9	0.083	*0.118*	0.296	*0.622*	*0.480*	*44*
31–Dec	IV-9	1	0.806	6.99	0.80	10.3	*10.3*	38.1	0.056	*0.083*	0.307	*0.531*	*0.275*	*34*
Wtd. mean			*0.771*	*6.93*	*0.81*	*9.6*	*8.59*	*38.7*	*0.060*	*0.078*	*0.261*	*0.523*	*0.370*	*40*
St. dev (unWtd.)			*0.475*	*1.03*	*0.14*	*0.6*	*2.70*	*10.9*	*0.025*	*0.048*	*0.163*	*0.248*	*0.235*	*11*
2003														
1–7 Jan	IV-9	7	0.806	6.99	0.80	10.3	*10.3*	38.1	0.056	*0.083*	0.307	*0.531*	*0.275*	*34*
8 Jan–23 Feb	IV-10	47	0.406	6.92	0.87	9.3	*13.6*	38.3	0.028	*0.055*	0.155	*0.281*	*0.125*	*31*
24–Feb		1	nd	nd	nd	nd	nd	nd	nd	nd	nd	nd	nd	
25 Feb–10 Mar	V-1	14	0.464	5.57	0.56	11.6	*11.2*	14.1	0.026	*0.052*	0.066	*0.182*	*0.282*	*61*
11–24 Mar	V-2	14	0.358	5.58	0.57	11.4	*12.1*	15.7	0.020	*0.043*	0.056	*0.149*	*0.208*	*58*
25 Mar–7 Apr [a]	V-3	14	0.652	5.83	nd	nd	*4.61*	23.2	0.038	*0.030*	0.151	*0.276*	*0.376*	*58*
8–21 Apr	V-4	14	0.715	6.04	0.77	9.2	*9.84*	28.5	0.043	*0.070*	0.204	*0.382*	*0.333*	*47*
22 Apr–5 May [a]	V-5	14	0.229	5.79	nd	nd	*9.91*	11.6	0.013	*0.023*	0.027	*0.082*	*0.146*	*64*
6–19 May [a]	V-6	14	0.225	6.51	nd	nd	*11.5*	21.8	0.015	*0.026*	0.049	*0.112*	*0.114*	*50*
20 May–2 Jun	V-7	14	0.531	7.65	0.90	9.9	*6.75*	44.3	0.041	*0.036*	0.235	*0.373*	*0.158*	*30*
3–16 Jun	V-8	14	0.580	6.29	0.74	10.0	*2.67*	50.1	0.036	*0.015*	0.291	*0.397*	*0.183*	*31*
17–30 Jun	V-9	14	0.749	6.49	0.76	9.9	*2.58*	54.2	0.049	*0.019*	0.406	*0.547*	*0.202*	*27*
1–14 Jul	V-10	14	0.617	8.34	1.05	8.6	*5.68*	49.2	0.051	*0.035*	0.304	*0.467*	*0.150*	*24*
15–27 Jul	V-11	13	0.431	9.24	1.04	10.4	*5.33*	31.9	0.040	*0.023*	0.138	*0.260*	*0.171*	*40*
28 Jul–9 Aug	V-12	13	0.422	8.34	0.93	10.4	*8.00*	27.7	0.035	*0.034*	0.117	*0.239*	*0.183*	*43*
10–21 Aug		12	nd	nd	nd	nd	nd	nd	nd	nd	nd	nd	nd	
22–28 Aug	VI-2	7	3.884	3.36	0.38	10.4	6.03	9.71	0.130	0.234	0.377	0.938	2.947	76
29 Aug–4 Sep	VI-3	7	3.322	3.59	0.38	11.0	8.92	9.10	0.119	0.296	0.302	0.896	2.426	73
05–11 Sep	VI-4	7	1.459	5.48	0.66	9.7	14.3	18.6	0.080	0.209	0.271	0.680	0.779	53
12–18 Sep	VI-5	7	0.808	7.09	0.82	10.1	14.6	26.4	0.057	0.118	0.213	0.474	0.334	41
19–25 Sep [a]	VI-6	7	2.891	4.30	nd	nd	10.6	11.3	0.124	0.308	0.328	0.947	1.944	67
26 Sep–3 Oct	VI-7	8	2.870	2.96	0.33	10.3	10.8	6.03	0.085	0.309	0.173	0.694	2.176	76
4 Oct–13 Nov		41	nd	nd	nd	nd	nd	nd	nd	nd	nd	nd	nd	
14–22 Nov	VII-1	9	0.999	6.05	0.70	10.0	14.9	18.7	0.060	0.149	0.187	0.487	0.512	51
23 Nov–1 Dec	VII-2	9	0.809	5.51	0.62	10.4	13.2	28.7	0.045	0.107	0.232	0.451	0.358	44
2–10 Dec	VII-3	9	1.565	5.20	0.66	9.2	12.4	42.2	0.081	0.194	0.661	1.059	0.506	32
11–19 Dec	VII-4	9	2.103	5.07	0.70	8.4	12.5	30.5	0.107	0.263	0.641	1.170	0.932	44
20–28 Dec	VII-5	9	1.183	6.10	0.77	9.3	14.6	48.1	0.072	0.172	0.568	0.921	0.261	22
29–31 Dec	VII-6	3	1.720	4.91	nd	nd	11.2	37.7	0.085	0.192	0.649	1.052	0.668	39
Wtd. mean			*0.907*	*6.29*	*0.77*	*10.0*	*9.88*	*30.0*	*0.050*	*0.090*	*0.232*	*0.444*	*0.463*	44
St. dev (unWtd.)			*1.020*	*1.50*	*0.20*	*0.8*	*3.69*	*14.3*	*0.034*	*0.101*	*0.184*	*0.325*	*0.793*	16
No Hur.			*0.688*	*6.58*	*0.83*	*10.3*	*9.95*	*32.1*	*0.043*	*0.070*	*0.226*	*0.401*	*0.268*	*41*
St. dev (unWtd.)			*0.504*	*1.15*	*0.14*	*0.8*	*3.92*	*12.6*	*0.001*	*0.075*	*0.198*	*0.315*	*0.223*	*12*
2004														
1–6 Jan	VII-6	6	1.720	4.91	nd	nd	11.2	37.7	0.085	0.192	0.649	1.052	0.668	39
7–15 Jan [a]	VII-7	9	0.711	5.89	0.70	9.9	11.4	58.9	0.042	0.081	0.419	0.605	0.106	15
16–24 Jan [a]	VII-8	9	0.380	6.93	nd	nd	9.31	62.3	0.026	0.035	0.237	0.338	0.042	11
25 Jan–2 Feb [a]	VII-9	9	0.295	7.65	nd	nd	12.2	49.4	0.023	0.036	0.146	0.238	0.057	19
3–11 Feb	VII-10	9	0.513	7.55	0.94	9.3	12.2	54.3	0.039	0.063	0.279	0.438	0.075	15
12–20 Feb	VII-11	9	1.058	7.59	1.03	8.6	10.5	54.8	0.080	0.111	0.579	0.891	0.167	16
21–29 Feb [a]	VII-12	9	0.299	8.25	nd	nd	8.92	51.1	0.025	0.027	0.153	0.242	0.058	19
1–10 Mar		10	nd	nd	nd	nd	nd	nd	nd	nd	nd	nd	nd	
11–25 Mar	VIII-1	15	0.605	8.98	1.18	8.9	15.0	30.6	0.054	0.091	0.185	0.412	0.193	32
26 Mar–9 Apr	VIII-2	15	0.418	8.78	1.15	8.9	18.8	21.1	0.037	0.079	0.088	0.259	0.159	38
10–24 Apr	VIII-3	15	0.371	9.79	1.29	8.8	10.2	43.8	0.036	0.038	0.163	0.291	0.080	22
25 Apr–9 May	VIII-4	15	0.391	10.1	1.29	9.2	7.99	49.8	0.040	0.031	0.194	0.325	0.066	17
10–24 May	VIII-5	15	0.202	16.4	2.14	8.9	7.92	25.4	0.033	0.016	0.051	0.150	0.052	26

25 May–8 Jun [a]	VIII-6	15	0.109	9.50	nd	nd	13.6	52.5	0.010	0.015	0.057	0.098	0.011	10
9 Jun–23 Sep		107	nd	nd	nd	nd	nd	nd	nd	nd	nd	nd	nd	
24 Sep–9 Oct	IX-1	16	0.726	9.04	1.23	8.6	16.4	15.7	0.066	0.119	0.114	0.398	0.328	45
10–26 Oct	IX-2	17	0.852	8.04	0.94	10.0	18.8	11.2	0.068	0.160	0.096	0.427	0.424	50
27 Oct–12 Nov	IX-3	17	0.965	6.73	0.80	9.9	19.3	11.6	0.065	0.186	0.112	0.460	0.504	52
13–28 Nov	IX-4	16	0.871	7.00	0.87	9.4	18.7	14.6	0.061	0.163	0.127	0.443	0.429	49
29 Nov–14 Dec	IX-5	16	2.245	4.46	0.54	9.7	13.5	23.9	0.100	0.303	0.536	1.090	1.155	51
15–24 Dec	IX-6	10	1.067	6.85	0.87	9.2	12.9	39.1	0.073	0.138	0.417	0.738	0.329	31
25–31 Dec	IX-7	7	0.900	6.33	0.77	9.6	15.7	29.0	0.057	0.141	0.261	0.545	0.355	39
Wtd. mean			*0.907*	*8.22*	*1.12*	*9.7*	*13.7*	*33.0*	*0.050*	*0.104*	*0.214*	*0.447*	*0.367*	*32*
St. dev (unWtd.)			*0.522*	*2.49*	*0.38*	*0.5*	*3.7*	*17.0*	*0.024*	*0.075*	*0.181*	*0.278*	*0.280*	*15*
2005														
1–3 Jan	IX-7	3	0.900	6.33	0.77	9.6	15.7	29.0	0.057	0.141	0.261	0.545	0.355	39
4–13 Jan	IX-8	10	0.399	7.43	0.89	9.8	12.3	30.0	0.030	0.049	0.120	0.243	0.156	39
14–23 Jan	IX-9	10	0.400	6.98	0.82	9.9	14.4	31.7	0.028	0.058	0.127	0.254	0.146	36
24 Jan–2 Feb [a]	IX-10	10	0.173	8.14	nd	nd	14.0	44.9	0.014	0.024	0.078	0.138	0.036	21
3–12 Feb [a]	IX-11	10	0.116	7.64	nd	nd	12.2	36.5	0.009	0.014	0.042	0.079	0.037	32
13–22 Feb [a]	IX-12	10	0.129	7.80	nd	nd	15.3	31.9	0.010	0.020	0.041	0.086	0.043	33
23–Feb		1	nd	nd	nd	nd	nd	nd	nd	nd	nd	nd	nd	
24 Feb–10 Mar	X-1	15	0.304	8.38	1.07	9.1	18.8	14.5	0.026	0.057	0.044	0.165	0.139	46
11–25 Mar	X-2	15	0.488	7.67	0.89	10.1	14.4	23.5	0.037	0.070	0.115	0.279	0.209	43
26 Mar–9 Apr	X-3	15	0.469	10.0	1.20	9.7	13.8	19.8	0.047	0.065	0.093	0.275	0.194	41
10–24 Apr	X-4	15	0.318	8.94	1.00	10.4	10.7	20.4	0.028	0.034	0.065	0.170	0.148	47
25 Ap –9 May	X-5	15	0.402	8.30	0.93	10.4	8.9	41.2	0.033	0.036	0.166	0.285	0.117	29
10–24 May	X-6	15	0.303	8.73	1.07	9.5	10.7	32.9	0.026	0.033	0.100	0.198	0.104	35
25 May–8 Jun	X-7	15	0.240	8.82	1.09	9.4	5.2	50.7	0.021	0.012	0.121	0.187	0.053	22
9–23 Jun	X-8	15	0.439	9.06	1.16	9.1	5.5	50.3	0.040	0.024	0.221	0.345	0.095	22
24Jun–8 Jul	X-9	15	0.252	9.88	1.28	9.0	8.0	35.6	0.025	0.020	0.090	0.172	0.080	32
9–23 Jul	X-10	15	0.345	10.8	1.37	9.2	8.4	29.2	0.037	0.029	0.101	0.223	0.122	35
24 Jul–7 Aug	X-11	15	0.194	9.74	1.27	8.9	12.5	23.7	0.019	0.024	0.046	0.118	0.077	39
8–22 Aug	X-12	15	0.288	9.51	1.19	9.3	12.3	17.5	0.027	0.036	0.050	0.154	0.134	46
23–Aug		1	nd	nd	nd	nd	nd	nd	nd	nd	nd	nd	nd	
24–31 Aug	XI-1	8	0.719	10.7	1.40	8.9	13.5	17.7	0.077	0.097	0.127	0.416	0.303	42
1–8 Sep	XI-2	8	0.867	8.70	1.09	9.3	17.3	10.1	0.075	0.150	0.087	0.426	0.441	51
9–16 Sep	XI-3	8	0.639	8.96	1.13	9.2	16.5	11.4	0.057	0.106	0.073	0.322	0.317	50
17–24 Sep	XI-4	8	0.655	10.0	1.22	9.6	16.2	11.9	0.066	0.106	0.078	0.348	0.307	47
25 Sep–2 Oct	XI-5	8	0.404	11.1	1.40	9.3	19.1	12.4	0.045	0.077	0.050	0.240	0.165	41
3–10 Oct	XI-6	8	0.500	9.60	1.16	9.6	18.0	9.60	0.048	0.090	0.048	0.258	0.242	48
11–18 Oct	XI-7	8	0.469	8.65	1.03	9.8	17.4	12.6	0.041	0.082	0.059	0.243	0.227	48
19–26 Oct	XI-8	8	0.737	9.32	1.12	9.7	18.8	14.2	0.069	0.139	0.105	0.415	0.322	44
27 Oct–3 Nov	XI-9	8	0.475	10.4	1.34	9.1	20.3	9.79	0.050	0.097	0.047	0.267	0.208	44
4–11 Nov [a]	XI-10	8	0.304	11.4	nd	nd	25.7	14.9	0.034	0.078	0.045	0.210	0.094	31
12–19 Nov [a]	XI-11	8	0.393	11.0	nd	nd	24.9	12.2	0.043	0.098	0.048	0.254	0.139	35
20–29 Nov	XI-12	10	0.657	7.30	0.93	9.2	18.6	17.6	0.048	0.122	0.116	0.358	0.300	46
30 Nov–1 Dec		2	nd	nd	nd	nd	nd	nd	nd	nd	nd	nd	nd	
2–15 Dec	XII-2	14	1.857	4.99	0.64	9.1	13.9	23.8	0.093	0.259	0.443	0.933	0.923	50
16–22 Dec	XII-3	7	0.512	6.70	0.81	9.6	15.2	24.0	0.034	0.078	0.123	0.287	0.225	44
23–29 Dec	XII-4	7	0.687	6.86	0.84	9.6	15.7	22.7	0.047	0.108	0.156	0.382	0.305	44
30–31 Dec	XII-5	2	0.299	8.78	1.07	9.6	10.4	28.4	0.026	0.031	0.085	0.182	0.117	39
Wtd. mean			*0.461*	*8.81*	*1.08*	*9.5*	*13.7*	*25*	*0.038*	*0.066*	*0.107*	*0.269*	*0.192*	*39*
St. dev (unWtd.)			*0.314*	*1.50*	*0.20*	*0.4*	*4.7*	*12*	*0.020*	*0.052*	*0.078*	*0.156*	*0.163*	*8*
2006														
1–5 Jan	XII-5	5	0.299	8.78	1.07	9.6	10.4	28.4	0.026	0.031	0.085	0.182	0.117	39
6–12 Jan	XII-6	7	0.786	7.24	0.94	9.0	8.86	40.2	0.057	0.070	0.316	0.528	0.259	33
13–19 Jan	XII-7	7	0.850	5.85	0.75	9.1	9.78	29.3	0.050	0.083	0.249	0.456	0.394	46
20–26 Jan	XII-8	7	2.287	3.73	0.50	8.7	16.3	20.4	0.085	0.373	0.466	1.052	1.235	54
27 Jan–2 Feb	XII-9	7	0.483	5.87	0.74	9.3	12.4	20.4	0.028	0.060	0.098	0.229	0.254	53
3–9 Feb	XII-10	7	0.133	nd	nd	nd	nd	18.4	nd	nd	nd	nd	nd	
10–16 Feb	XII-11	7	0.524	6.98	0.91	8.9	11.2	28.7	0.037	0.059	0.150	0.300	0.223	43
17–23 Feb	XII-12	7	0.423	nd	nd	nd	nd	47.0	nd	nd	nd	nd	nd	
24 Feb–19 Sep		208	nd	nd	nd	nd	nd	nd	nd	nd	nd	nd	nd	
20 Sep–1 Oct	XIV-1	12	1.127	8.75	1.17	8.7	15.2	13.2	0.099	0.171	0.149	0.566	0.560	50
2–13 Oct	XIV-2	12	0.775	8.50	1.07	9.3	15.3	10.5	0.066	0.119	0.082	0.365	0.410	53
14–25 Oct	XIV-3	12	0.530	9.58	1.18	9.4	16.1	10.3	0.051	0.085	0.055	0.267	0.263	50

26 Oct–6 Nov	XIV-4	12	0.764	8.35	1.00	9.7	16.5	9.3	0.064	0.126	0.071	0.357	0.407	53
7 Nov–31 Dec	XIV–5	55	0.428	4.80	0.59	9.5	20.0	15.9	0.021	0.086	0.068	0.205	0.223	52
Wtd. mean			*0.648*	*6.56*	*0.82*	*9.3*	*16.2*	*18.7*	*0.045*	*0.108*	*0.121*	*0.341*	*0.343*	*50*
St. dev (unWtd.)			*0.538*	*1.87*	*0.23*	*0.4*	*3.5*	*10.0*	*0.025*	*0.094*	*0.130*	*0.248*	*0.304*	*6*
2007														
1 Jan–17 Feb		48	0.428	4.80	0.59	9.5	20.0	15.9	0.021	0.086	0.068	0.205	0.223	52
18–24 Feb	XV-1	7	0.630	9.04	1.24	8.5	13.8	31.0	0.057	0.087	0.196	0.425	0.206	33
25 Feb–3 Mar	XV-2	7	0.639	8.42	1.14	8.6	14.2	22.6	0.054	0.091	0.145	0.370	0.269	42
4–10 Mar	XV-3	7	1.127	6.50	0.85	8.9	13.7	21.4	0.073	0.154	0.242	0.579	0.548	49
11–17 Mar	XV-4	7	0.703	7.65	0.99	9.0	17.7	23.8	0.054	0.124	0.167	0.426	0.277	39
18–24 Mar	XV-5	7	0.601	8.17	1.05	9.1	18.1	24.3	0.049	0.109	0.146	0.378	0.223	37
25–31 Mar	XV-6	7	0.734	8.08	1.03	9.2	17.0	29.2	0.059	0.125	0.214	0.488	0.246	34
1–7 Apr	XV-7	7	0.483	8.30	1.04	9.3	18.6	25.2	0.040	0.090	0.122	0.312	0.171	35
8–13 Apr	XV-8	7	0.308	8.63	1.07	9.4	14.8	25.1	0.027	0.046	0.077	0.189	0.119	39
15–21 Apr	XV-9	7	0.241	8.72	1.08	9.4	16.1	24.0	0.021	0.039	0.058	0.149	0.092	38
22–28 Apr	XV-10	7	0.305	9.56	1.23	9.0	10.5	44.8	0.029	0.032	0.137	0.241	0.063	21
29 Apr–5 May	XV-11	7	0.347	9.93	1.30	8.9	11.3	38.4	0.034	0.039	0.133	0.259	0.089	25
6–11 May	XV-12	6	0.174	10.9	1.43	8.9	10.7	30.4	0.019	0.019	0.053	0.119	0.055	32
12–May		1	nd	nd	nd	nd	nd	nd	nd	nd	nd	nd	nd	
13–27 May	XVI-1	15	0.416	7.87	1.05	8.7	14.9	16.4	0.033	0.062	0.068	0.212	0.204	49
28 May–12 Jun	XVI-2	15	0.906	9.17	1.23	8.7	7.94	26.5	0.083	0.072	0.240	0.520	0.386	43
12–26 Jun	XVI-3	15	0.633	9.47	1.31	8.5	12.1	18.7	0.060	0.077	0.118	0.345	0.288	46
27 Jun–11 Jul	XVI-4	15	0.477	10.5	1.41	8.7	7.65	25.0	0.050	0.036	0.119	0.280	0.197	41
12–26 Jul	XVI-5	15	0.596	9.32	1.24	8.7	9.28	26.8	0.056	0.055	0.160	0.354	0.242	41
27Jul–11 Aug	XVI-6	16	0.471	9.46	1.30	8.5	11.4	18.0	0.045	0.054	0.085	0.250	0.221	47
12–27 Aug	XVI-7	16	0.489	13.6	1.81	8.7	10.3	15.6	0.066	0.051	0.076	0.292	0.196	40
28 Aug–12 Sep	XVI-8	16	1.947	7.48	0.92	9.4	17.3	10.9	0.146	0.338	0.213	0.914	1.032	53
13–28 Sep	XVI-9	16	0.396	7.19	0.89	9.4	18.8	10.5	0.028	0.075	0.041	0.187	0.209	53
29 Sep–14 Oct	XVI-10	16	0.397	8.40	1.04	9.4	14.9	8.87	0.033	0.059	0.035	0.178	0.219	55
15–30 Oct	XVI-11	16	0.530	6.49	0.82	9.2	17.3	7.22	0.034	0.092	0.038	0.216	0.314	59
31 Oct–14 Nov	XVI-12	15	0.310	7.86	1.07	8.6	17.8	10.2	0.024	0.055	0.031	0.148	0.162	52
15–Nov		1	nd	nd	nd	nd	nd	nd	nd	nd	nd	nd	nd	
16–23 Nov	XVII-1	8	0.896	8.37	1.07	9.1	15.1	20.2	0.075	0.135	0.181	0.504	0.393	44
24 Nov–1 Dec	XVII-2	8	1.404	6.03	0.78	9.0	22.3	15.3	0.085	0.312	0.214	0.738	0.666	47
2–9 Dec	XVII-3	8	0.647	6.24	0.77	9.4	19.7	14.8	0.040	0.128	0.096	0.324	0.323	50
10–17 Dec	XVII-4	8	1.624	5.87	0.78	8.7	17.2	14.9	0.095	0.279	0.242	0.759	0.865	53
18–25 Dec	XVII-5	8	4.541	3.88	0.55	8.3	14.9	18.3	0.176	0.678	0.831	1.949	2.592	57
26–31 Dec		6	2.915	4.14	0.56	8.7	11.1	21.1	0.121	0.322	0.614	1.238	1.677	58
Wtd. mean			*0.751*	*7.85*	*1.03*	*9.0*	*15.0*	*19.0*	*0.053*	*0.113*	*0.138*	*0.384*	*0.367*	*46*
St. dev (unWtd.)			*0.891*	*2.00*	*0.27*	*0.4*	*3.8*	*8.5*	*0.037*	*0.134*	*0.165*	*0.374*	*0.522*	*10*
2008														
1–2 Jan	XVII-6	2	2.915	4.14	0.56	8.7	11.1	21.1	0.121	0.322	0.614	1.238	1.677	58
3–10 Jan	XVII-7	8	1.480	4.72	0.65	8.5	10.9	15.4	0.070	0.161	0.227	0.563	0.917	62
11–17 Jan	XVII-8	7	0.639	6.28	0.84	8.7	8.2	22.3	0.040	0.052	0.142	0.295	0.344	54
18–24 Jan	XVII-9	7	1.203	5.29	0.71	8.7	9.2	23.0	0.064	0.110	0.277	0.546	0.656	55
25–31 Jan	XVII-10	7	0.694	6.89	0.95	8.5	7.1	24.8	0.048	0.049	0.172	0.340	0.353	51
1–7 Feb	XVII-11	7	0.618	7.07	1.02	8.1	9.8	18.1	0.044	0.060	0.112	0.282	0.336	54
8–14 Feb	XVII-12	7	0.628	6.44	0.90	8.4	10.4	18.6	0.040	0.065	0.117	0.283	0.345	55
15–Feb		1	nd	nd	nd	nd	nd	nd	nd	nd	nd	nd	nd	
16–25 Feb	XVIII-1	10	0.491	7.29	1.05	8.1	11.1	26.4	0.036	0.054	0.130	0.273	0.217	44
26 Feb –5 Mar	XVIII-2	9	0.616	8.29	1.17	8.2	11.1	28.4	0.051	0.068	0.175	0.371	0.245	40
6–14 Mar	XVIII-3	9	0.354	12.3	1.85	7.7	11.5	32.0	0.043	0.041	0.113	0.262	0.092	26
15–23 Mar	XVIII-4	9	0.209	12.2	1.83	7.8	11.6	37.1	0.026	0.024	0.078	0.166	0.043	21
24 Mar–1 Apr	XVIII-5	9	0.405	10.5	1.46	8.4	6.9	25.0	0.042	0.028	0.101	0.235	0.170	42
2–10 Apr	XVIII-6	9	0.365	13.1	1.85	8.3	8.6	32.1	0.048	0.031	0.117	0.268	0.097	27
11–18 Apr	XVIII-7	8	0.623	10.7	1.48	8.5	7.2	26.5	0.067	0.045	0.165	0.377	0.246	39
19–26 Apr	XVIII-8	8	0.743	11.5	1.65	8.1	8.0	24.8	0.085	0.060	0.184	0.457	0.286	38
27 Apr–4 May	XVIII-9	8	0.118	13.4	1.97	7.9	9.1	34.1	0.016	0.011	0.040	0.091	0.028	23
5–12 May	XVIII-10	8	0.337	11.9	1.75	7.9	11.8	18.3	0.040	0.040	0.062	0.202	0.135	40
13–20 May	XVIII-11	8	0.062	16.1	2.40	7.8	11.1	29.0	0.010	0.007	0.018	0.050	0.012	19
21–28 May	XVIII-12	7.5	0.812	10.6	1.50	8.2	8.0	27.9	0.086	0.065	0.227	0.507	0.305	38
28-May		0.5	nd	nd	nd	nd	nd	nd	nd	nd	nd	nd	nd	
29 May–10 Jun	XIX-1	13	0.432	13.1	1.95	7.8	3.6	44.2	0.057	0.015	0.191	0.348	0.084	19
11–23 Jun	XIX-2	13	0.043	nd	nd	nd	nd	32.8	nd	nd	nd	nd	nd	

24 Jun–6 Jul	XIX-3	13	nd	nd	nd	nd	nd	nd	nd	nd	nd	nd	nd	
7–19 Jul	XIX-4	13	nd	nd	nd	nd	nd	nd	nd	nd	nd	nd	nd	
20 Jul–1 Aug	XIX-5	13	nd	nd	nd	nd	nd	nd	nd	nd	nd	nd	nd	
2–14 Aug	XIX-6	13	nd	nd	nd	nd	nd	nd	nd	nd	nd	nd	nd	
15–27 Aug	XIX-7	13	nd	nd	nd	nd	nd	nd	nd	nd	nd	nd	nd	
28 Aug–9 Sep	XIX-8	13	nd	nd	nd	nd	nd	nd	nd	nd	nd	nd	nd	
10–22 Sep	XIX-9	13	0.087	15.6	2.19	8.3	4.4	32.2	0.014	0.004	0.028	0.066	0.021	24
23 Sep–4 Oct	XIX-10	12	nd	nd	nd	nd	nd	nd	nd	nd	nd	nd	nd	
5–16 Oct	XIX-11	12	nd	nd	nd	nd	nd	nd	nd	nd	nd	nd	nd	
17–29 Oct	XIX-12	13	nd	nd	nd	nd	nd	nd	nd	nd	nd	nd	nd	
30–Oct		0.5	nd	nd	nd	nd	nd	nd	nd	nd	nd	nd	nd	
31 Oct–11 Nov	XX-1	12	0.945	8.03	1.45	6.5	16.8	21.1	0.076	0.159	0.200	0.548	0.397	42
12–23 Nov	XX-2	12	1.071	6.58	1.23	6.2	15.7	16.4	0.070	0.168	0.176	0.520	0.551	51
24 Nov–5 Dec	XX-3	12	1.138	7.96	1.58	5.9	13.5	19.2	0.091	0.154	0.219	0.598	0.539	47
6–17 Dec	XX-4	12	1.387	5.44	1.12	5.7	15.6	14.7	0.075	0.216	0.204	0.608	0.778	56
18–29 Dec	XX-5	12	0.946	6.19	1.05	6.9	13.4	16.9	0.059	0.127	0.160	0.434	0.512	54
30–31 Dec	XX-6	2	0.980	7.18	1.16	7.2	13.3	17.7	0.070	0.130	0.173	0.480	0.501	51
Wtd. mean			*0.655*	*9.50*	*1.44*	*7.7*	*10.4*	*25.6*	*0.053*	*0.080*	*0.144*	*0.364*	*0.325*	*41*
St. dev (unWtd.)			*0.582*	*3.42*	*0.49*	*0.9*	*3.2*	*7.3*	*0.026*	*0.075*	*0.112*	*0.231*	*0.352*	*13*
2009														
1–10 Jan	XX-6	12	0.980	7.18	1.16	7.2	13.3	17.7	0.070	0.130	0.173	0.480	0.501	51
11–22 Jan	XX-7	12	3.380	4.66	0.95	5.7	12.0	18.6	0.157	0.405	0.629	1.428	1.952	58
23 Jan–3 Feb	XX-8	12	0.911	6.05	1.11	6.4	9.6	17.2	0.055	0.087	0.157	0.382	0.529	58
4–15 Feb	XX-9	12	0.626	7.68	1.28	7.0	9.6	16.1	0.048	0.060	0.101	0.281	0.345	55
16–27 Feb	XX-10	12	1.014	7.39	1.28	6.7	6.8	38.2	0.075	0.069	0.388	0.643	0.371	37
28 Feb–11 Mar	XX-11	12	0.239	10.4	1.78	6.8	7.5	17.7	0.025	0.018	0.042	0.122	0.117	49
12–24 Mar	XX-12	13	0.174	12.3	2.17	6.6	7.5	9.6	0.021	0.013	0.017	0.083	0.091	52
25–Mar-3 Apr		10	nd	nd	nd	nd	nd	nd	nd	nd	nd	nd	nd	
4–18 Apr	XXI-1	15	0.406	16.6	2.79	7.0	10.2	15.4	0.067	0.041	0.062	0.272	0.133	33
19 Apr–3 May	XXI-2	15	0.227	16.8	2.69	7.3	9.9	17.3	0.038	0.022	0.039	0.157	0.070	31
4–18 May	XXI-3	15	0.231	11.1	1.75	7.4	9.3	21.8	0.026	0.021	0.050	0.135	0.095	41
19 May–2 Jun	XXI-4	15	0.898	10.6	1.69	7.4	9.7	17.9	0.096	0.087	0.161	0.487	0.411	46
3–17 Jun	XXI-5	15	0.497	10.7	1.75	7.2	9.4	26.2	0.053	0.047	0.130	0.310	0.187	38
18 Jun–2 Jul	XXI-6	15	0.898	10.5	1.68	7.3	6.4	27.3	0.094	0.057	0.245	0.537	0.362	40
3–17 Jul	XXI-7	15	0.366	11.1	1.79	7.2	9.6	25.7	0.041	0.035	0.094	0.231	0.135	37
18 Jul–1 Aug	XXI-8	15	0.673	9.83	1.59	7.2	12.0	19.1	0.066	0.081	0.128	0.375	0.298	44
2–16 Aug	XXI-9	15	0.409	10.3	1.56	7.7	13.6	15.6	0.042	0.056	0.064	0.225	0.184	45
17–31 Aug	XXI-10	15	0.256	12.8	1.91	7.8	13.8	13.0	0.033	0.035	0.033	0.151	0.105	41
1–15 Sep	XXI-11	15	0.143	11.8	1.73	8.0	14.5	13.1	0.017	0.021	0.019	0.082	0.061	43
16–18 Sep		3	nd	nd	nd	nd	nd	nd	nd	nd	nd	nd	nd	
19 Sep–3 Oct	XXII-1	15	0.078	10.3	nd	nd	nd	18.7	nd	nd	0.015	nd	nd	
4–18 Oct	XXII-2	15	0.219	10.8	nd	nd	nd	8.9	0.023	nd	0.019	nd	nd	
19 Oct–2 Nov	XXII-3	15	0.227	6.6	nd	nd	nd	9.8	0.024	nd	0.022	nd	nd	
3–17 Nov	XXII-4	15	0.067	6.6	nd	nd	nd	13.3	0.004	nd	0.009	nd	nd	
18 Nov–2 Dec	XXII-5	15	0.346	8.1	nd	nd	nd	21.7	0.023	nd	0.075	nd	nd	
3–17 Dec	XXII-6	15	0.244	7.0	nd	nd	nd	26.7	0.020	nd	0.065	nd	nd	
18–31 Dec	XXII-7	14	0.198	nd	nd	nd	nd	27.5	0.014	nd	0.054	nd	nd	
Wtd. mean			*0.516*	*7.9*	*1.74*	*7.1*	*10.3*	*18.9*	*0.041*	*0.067*	*0.134*	*0.341*	*0.309*	*44*
St. dev (unWtd.)			*0.662*	*3.0*	*0.49*	*0.5*	*2.5*	*6.8*	*0.034*	*0.089*	*0.138*	*0.314*	*0.432*	*8*

nd = no data; is= insufficient sample.
Note: *small italic numbers* (Jan 2002–Aug 2003) reflect underestimates of $CaCO_3$.
Corg = organic carbon; N = Nitrogen; BioSi = biogenic silica; Biogen = biogenic fraction; Litho = lithogenic fraction.
Wtd. mean = Weighted for the number of days for each sample.
No Hur. = Ignores samples influenced by hurricanes "Ignacio" (24 Aug) and "Marty" (21 Sep).

[a] Carbon values extrapolated via linear regression

References

Aguiñiga, S., Sanchez, A., Silverberg, N., 2010. Temporal variations of C, N, $\delta^{13}C$, and $\delta^{15}N$ in organic matter collected by a sediment trap at Cuenca Alfonso, Bahía de La Paz, SW Gulf of California. Cont. Shelf Res. 30, 1692–1700.

Aguirre-Bahena, F., 2007. Cambios temporales en los componentes y los flujos de la materia en hundimiento en Cuenca Alfonso, Bahía de La Paz, durante el periodo 2002–2005. Doctoral Thesis. Centro Interdisciplinario de Ciencias Marinas-IPN. 104p.

Alldredge, A.L., Silver, M.W., 1988. Characteristics, dynamics, and significance of marine snow. Prog. Oceanogr. 20, 41–82.

Alvarez-Borrego, S., Schwartzlose, R.A., 1979. Water masses of the Gulf of California. Cienc. Mar 6, 41–59.

Alvarez-Borrego, S., Lara-Lara, J.R., 1991. The physical environment and primary productivity of the Gulf of California. In: Dauphin, J.P., Simoneit, B.R.T. (Eds.), The Gulf and Peninsular Province of the Californias. American Association of Petroleum Geologists, Tulsa, OK, pp. 555–567.

Armstrong, R.A., Lee, C., Hedges, J.I., Honjo, S., Wakeham, S.G., 2002. A new, mechanistic model for organic carbon fluxes in the ocean based on the

quantitative association of POC with ballast minerals. Deep Sea Res. Part II 49, 219–236.
Armstrong, R.A., Peterson, M.L., Lee, C., Wakeham, S.G., 2009. Settling velocity spectra and the ballast ratio hypothesis. Deep Sea Res. Part II 56, 1470–1478.
Badan-Dangon, A., Dorman, C.E., Merrifield, M.A., Winant, C.D., 1991. The lower atmosphere over the Gulf of California. J. Geophys. Res. 96, 16,877–16,896.
Bagnold, R.A., 1941. The Physics of Blown Sand and Desert Dunes. Methuen, London.
Behrenfeld, M.J., Falkowski, P.G., 1997. Photosynthetic rates derived from satellite-based chlorophyll concentration. Limnol. Oceanogr. 42, 1–20.
Buesseler, K.O., Antia, A.N., Chen, M., Fowler, S.W., Gardner, W.D., Gustafsson, O., Harada, K., Anthony, F., Michaels, A.F., Rutgers van der Loeff, M., Sarin, M., Steinberg, D.K., Trull, T., 2007. An assessment of the use of sediment traps for estimating upper ocean particle fluxes. J. Mar. Res. 65, 345–416.
Castro, R., Durazo, R., Mascarenhas, A.S., Collins, C.A., Trasviña, T., 2006. Thermohaline variability and geostrophic circulation in the southern portion of the Gulf of California. Deep Sea Res. Part I 53, 188–200.
Cervantes-Duarte, R., Verdugo-Díaz, G., Váldez-Holguin, J-E., 2005. Model estacional de producción primaria mediante flourescencia natural en una región costera de Golfo de California, México. Hidrobiológica 15, 79–87.
Choumiline, K., 2011. Geoquímica de la materia particulada en hundimiento, y de los sedimentos recientes de Cuenca Alfonso, Bahía de La Paz. M.Sc. Thesis. Centro Interdisciplinario de Ciencias Marinas-IPN. 143 pp.
Cruz-Orozco, R., Martínez-Noriega, C., Mendoza-Maravillas, A., 1996. Batimetría y sedimentos de Bahía de La Paz, B.C.S., México. Océanides 11, 21–27.
De La Rocha, C.L., Nowald, N., Passow, U., 2008. Interactions between diatom aggregates, minerals, particulate organic carbon, and dissolved organic matter: further implications for the ballast hypothesis. Global Biogeochem. Cycles 22, GB4005, http://dx.doi.org/10.1029/2007GB003156.
DeMaster, D.J., 1981. The supply and accumulation of silica in the marine environment. Geochim. Cosmochim. Acta 45, 1715–1732.
Deuser, W.G., 1986. Seasonal and interannual variations in deep-water particle Xuxcs in the Sargasso Sea and their relation to surface hydrography. Deep Sea Res 33, 125–216.
Deuser, W.G., Jickells, T.D., King, P., Commeau, J.A., 1995. Decadal and annual changes in biogenic opal and carbonate fluxes to the deep Sargasso Sea. Deep Sea Res. Part I 42, 1923–1932.
Dugdale, R.C, Goering, J.J., 1967. Uptake of new and regenerated forms of nitrogen in primary productivity. Limnol. Oceanogr. 12, 196–206.
Dunne, J.P., Armstrong, R.A., Gnanadesikan, A., Sarmiento, J.L., 2005. Empirical and mechanistic models for the particle export ratio. Global Biogeochem. Cycles 19, GB4026, http://dx.doi.org/10.1029/2004GB002390.
Elskens, M., Brion, N., Buesseler, K., Van Mooy, B.A.S., Boyd, P., Dehairs, F., Savoye, N., Baeyens, W., 2008. Primary, new and export production in the NW Pacific subarctic gyre during the vertigo K2 experiments. Deep Sea Res. Part II 55, 1594–1604.
Emerson, S., Meking, S., Abell, J., 2001. The nutrient pump in the North Pacific ocean: nutrient sources, Redfield ratios and recent changes. Global Biogeochem. Cycles 15, 535–554.
Engel, A., Szlosek, J., Abramson, L., Liu, Z., Stewart, G., Hirschberg, D., Lee, C., 2009a. Investigating the effect of ballasting by $CaCO_3$ in Emiliana huxleyi, I. Formation, settling velocities, and physical properties of aggregates. Deep Sea Res. Part II 56, 1396–1407.
Engel, A., Abramson, Szlosek, J.L., Liu, Z., Stewart, G., Hirschberg, D., Lee, C., 2009b. Investigating the effect of ballasting by $CaCO_3$ in *Emiliana huxleyi*, II. Decomposition of particulate organic matter. Deep Sea Res. Part II 56, 1408–1419.
Eppley, R.W., Peterson, B.J., 1979. Particulate organic matter flux and planktonic new production in the deep ocean. Nature 282, 677–680.
Figueroa, M., Marinone, S.G., Lavin, M., 2003. Geostrophic gyres of the Gulf of California. In: Velasco Fuentes, O.U., Sheinbaum, J., Ochoa de la Torre, J.L. (Eds.), Nonlinear Processes in Geophysical Fluid Dynamics. Kluwer Academic Publishers, Dordrecht, The Netherlands, pp. 237–255.
Fischer, G., Wefer, G., Romero, O., Dittert, N., Ratmeyer, V., Donner, B., 2003. Transfer of particles into the deep Atlantic and the global ocean: control of nutrient supply and ballast production. In: Wefer, G., Mulitza, S., Ratmeyer, V. (Eds.), The South Atlantic in the Late Quaternary: reconstruction of Material Budgets and Current Systems. Springer-Verlag, Berlin, pp. 12–46.
Francois, R., Honjo, S., Krischfield, R., Manganini, S., 2002. Factors controlling the flux of organic carbon to the bathypelagic zone of the ocean. Global Biogeochem. Cycles 16 (4), 1087, http://dx.doi.org/10.1029/2001GB001722.
Gonzalez, H.E., Ortiz, V.C., Sobarzo, M., 2000. The role of faecal material in the particulate organic carbon flux in the northern Humboldt Current, Chile (23° S), before and during the 1997-1998 El Niño. J. Plankton Res. 22, 499–529.
Hausback, B., 1984. Cenozoic volcanic and tectonic evolution of Baja California Sur, Mexico. In: Frizzell, V.A. (Ed.), Geology of The Baja California Peninsula. Pacific Section Society of Economic Paleontologists and Mineralogists, Los Angeles, pp. 219–236.
Helm, P.J., Breed, C.S., 1999. Instrumented field studies of sediment transport by wind, U.S. Geological Survey Professional Paper 1598-B. In: Breed, C.S., Reheis, M.C. (Eds.), Desert Winds: Monitoring Wind-Related Surface Processes in Arizona. United States Government Printing Office, New Mexico, and California, pp. 31–51.
Honjo, S., Dymond, J., Prell, W., Ittekkot, V., 1999. Monsoon-controlled export fluxes to the interior of the Arabian Sea. Deep Sea Res. Part II 46, 1859–1902.
Iversen, M.H., Ploug, H., 2010. Ballast minerals and the sinking carbon flux in the ocean: carbon-specific respiration rates and sinking velocity of marine snow aggregates. Biogeosciences 7, 2613–2624.
Jiménez-Illescas, A., Obeso-Nieblas, R.M., Salas-De-León, D.A., 1997. Oceanografía física de la Bahía de la Paz, B.C.S.. In: Ramírez, Urbán, Ramírez-Rodríguez, J. y M. (Eds.), La Bahía de La Paz, Investigaciones y Conservación. U.A.B.C.S., p. 345.
Kahru, M., Marinone, S.G., Lluch-Cota, S.E., Parés-Sierra, A., Greg Mitchell, B., 2004. Ocean-color variability in the Gulf of California: scales from days to ENSO. Deep Sea Res. Part II 51, 139–146.
Karl, D., Christian, J., Dore, J., Hebel, D., Letelier, R., Tupas, L., Winn, C., 1996. Seasonal and interannual variability in primary production and particle flux at Station ALOHA. Deep Sea Res. Part II 43, 539–568.
Klaas, C., Archer, D.E., 2002. Association of sinking organic matter with various types of mineral ballast in the deep sea: implications for the rain ratio. Global Biogeochem. Cycles 16, GB1116, http://dx.doi.org/10.1029/2001GB001765.
Lampitt, R., Anitia, A., 1997. Particle flux in deep seas: regional characteristics and temporal variability. Deep Sea Res. Part I 44, 1377–1403.
Lavin, M.F., Marinone, S.G., 2003. An overview of the physical oceanography of the Gulf of California. In: Velasco-Fuentes, O.U., Sheinbaum, J., Ochoa, J. (Eds.), Nonlinear Processes in Geophysical Fluid Dynamics. Kluwer Academic Publishers, Amsterdam, pp. 173–204.
Laws, E.A., Falkowski, P.G., Smith, W.O., Ducklow, H., McCarthy, J.J., 2000. Temperature effects on export production in the open ocean. Global Biogeochem. Cycles 14, 1231–1246.
Lee, C., Peterson, M.L., Wakeham, S.G., Armstrong, R.A., Cochran, J.K., Miquel, J-C., Fowler, S., Hirschberg, D., Beck, A., Xue, J., 2009. Particulate organic matter and ballast fluxes measured using in time-series and settling velocity sediment traps in the northwestern Mediterranean Sea. Deep Sea Res. Part II 56, 1420–1436.
Ljutsarev, A.V., 1987. Determination of organic carbon in sea bottom sediments by dry combustion. Oceanology 26, 533–536.
Lluch-Cota, S.E., Parés-Sierra, A., Magaña-Rueda, V.O., Arreguín-Sánchez, F., Bazzino, G., Herrera-Cervantes, H., Lluch-Belda, D., 2010. Changing climate in the Gulf of California. Progr. Oceanogr 87, 114–126.
Lluch-Cota, D.B., Teniza-Guillén, G., 2000. BAC versus áreas adyacentes de la variabilidad interanual de pigmentos fotosintéticos a partir del Coastal Zone Color Scanner (CZCS). In: Lluch-Belda, D., Elorduy-Garay, J, Lluch-Cota, SE, Ponce-Díaz, G (Eds.), BAC, Centros de Actividad Biológica del Pacífico Mexicano, 1ª Edic. Centro de investigaciones Biológicas del Noroeste, S.C., La Paz, pp. 198–218.
Lutz, M., Dunbar, R., Caldeira, K., 2002. Regional variability in the vertical flux of particulate organic carbon in the ocean interior. Glob. Biogeochem. Cycles 16, 1037–1055.
Lutz, M., Caldeira, K., Dunbar, R., Behrenfeld, M.J., 2007. Seasonal rhythms of net primary production and particulate organic carbon flux describe biological pump efficiency in the global ocean. J. Geophys. Res. 112, C10011, http://dx.doi.org/10.1029/2006JC003706.
Machain-Castillo, M.A., Gío-Argáez, F.R., Thunell, R., Tappa, E., González-Chávez, G., Cuesta-Castillo, L.B., 2009. Flujos de masa total y carbon en el Golfo de Tehuantepec associados a surgencias durante el period de Febrero del 2006 a Febrero de 2007. Abstract in: Simposio Internacional del Carbon en México, Ensenada, 7–9 October, sponsored by PMC, INE, CICESE, UABC.
Marinone, S.G., Parés-Sierra, A., Castro, R., Mascarenhas, A., 2004. Correction to temporal and spatial variation of the surface winds in the Gulf of California. Geophys. Res. Lett. 31, L10305.
Martin, J., Knauer, G., Karl, D., Broenkow, W., 1987. VERTEX: carbon cycling in the northeast Pacific. Deep Sea Res. Part A 34, 267–286.
Martínez-López, A., Cervantes-Duarte, R., Reyes-Salinas, A., Valdez-Holguín, J.E., 2001. Cambio estacional de clorofila a en La Bahía de La Paz, B.C.S., México. Hidrobiológica 11 (1), 45–52.
Martínez-López, A., Álvarez-Gómez, I.G., Durazo, R., 2012. Climate Variability and Silicoflagellate Fluxes in Alfonso Basin (Southern Gulf of California). Botanica Marina, Walter de Gruyter, Berlin, Boston, http://dx.doi.org/10.1515/bot-2012-0101.
Merrifield, M.A., Winant, C.D., 1989. Shelf circulation in the Gulf of California: a description of the variability. J. Geophys. Res. 94, 18133–18160.
Monreal-Gómez, M.A., Molina-Cruz, A., Salas-de-Leon, D.A., 2001. Water masses and cyclonic circulation in Bay of La Paz, during June 1988. J. Mar. Syst 30, 305–315.
Montes, E., Muller-Kargar, F., Thunell, R., Hollander, D., Astor, Y., Varela, R., Soto, I., Lorenzoni, L., 2012. Vertical fluxes of particulatebiogenic material through the euphotic and twilight zones in the Cariaco Basin. Venezuela. Deep Sea Res. I 67, 73–84.
Mortlock, R., Froelich, P., 1989. A simple method for the rapid determination of biogenic opal in pelagic marine sediments. Deep Sea Res. Part A 36, 1415–1426.
Nava-Sánchez, E.H., 1997. Modern Fan Deltas of the West Coast of the Gulf of California, Mexico. Ph.D. Thesis. University of Southern California, Los Angeles.
Obeso-Nieblas, M., Shirasago, B., Sánchez-Velasco, L., Gaviño-Rodríguez, H., 2004. Hydrographic variability in Bahía de La Paz, B. C. S., Mexico, during the 1997–1998 El Niño. Deep Sea Res. Part II 51, 689–710.
Otosaka, S., Noriki, S., 2005. Relationship between composition of settling particles and organic carbon flux in the western North Pacific and the Japan Sea. J. Oceanogr. 61, 25–40.
Pardo, M.A., Silverberg, N., Gendron, D., Beier, E., Palacios, D.M., 2013. The role of environmental seasonality in the structure of a cetacean community in the southwester Gulf of California. Mar. Ecol. Prog. Ser. 487, 245–260, http://dx.doi.org/10.3354/meps10217.
Parés-Sierra, A., Mascarenhas, A., Marinone, S.G., Castro, R., 2003. Temporal and spatial variation of the surface winds in the Gulf of California. Geophys. Res. Lett. 30 (6), 1312, http://dx.doi.org/10.1029/2002GL016716.
Passow, U., 2004. Switching perspectives: do mineral fluxes determine particulate organic carbon fluxes or vice versa? Geochem. Geophys. Geosyst. 5, Q04002, http://dx.doi.org/10.1029/2003GC000670.

Passow, U., Shipe, R.F.., Murray, A., Pak, D.K., Brzezinski, M.A., Alldredge, A.L., 2001. The origin of transparent exopolymer particles (TEP) and their role in the sedimentation of particulate matter. Cont. Shelf Res. 21, 327–346, http://dx.doi.org/10.1016/S0278-4343(00)00101-1.

Passow, U., De La Rocha, C.L., 2006. The accumulation of mineral ballast on organic aggregates. Global Biogeochem. Cycles 20, GB1013 (doi).

Pérez-Cruz, L.L., 2000. Estudio paleoceanográfico y sedimentológico Holocénico de la Bahía de La Paz, Golfo de California. Tesis de Doctorado. Universidad Nacional Autónoma de México.

Pérez-Cruz, L., 2006. Climate and ocean variability during the middle and late Holocene recorded in laminated sediments from Alfonso Basin, Gulf of California, Mexico. Quat. Res 65, 401–410.

Reyes-Salinas, A., Cervantes-Duarte, R., Morales-Peréz, R.A., Valdez-Holguín, J.E., 2003. Variabilidad estacional de la productividad primaria y su relación con la estratificación vertical en la Bahía de La Paz, B.C.S. Seasonal variability of primary productivity and its relation to the vertical stratification in La Paz Bay, B.C.S. Hidrobiológica 13, 103–110.

Rodriguez Castañeda, A.P., 2008. Variación de flujos de los elementos particulada en Cuenca Alfonso, Bahía de La Paz, en el periodo 2002–2005. Doctoral Thesis. Centro Interdisciplinario de Ciencias Marinas—IPN. 199 p.

Roy, S., Silverberg, N., Romero, N., Deibel, D., Klein, B., Savenkoff, C., Vézina, A., Tremblay, J-E., Legendre, L., Rivkin, R.B., 2000. The impact of mesozooplankton feeding on the downward flux of biogenic carbon in the Gulf of St. Lawrence (Canada). Deep Sea Res. Part II 47, 515–544.

Salinas-González, F., Zaitsev, O., Makarov, V.G., 2003. Formación de la estructura termohalina del agua de la Bahía de La Paz de verano a otoño. Cienc. Mar 29, 51–65.

Sánchez-Velasco, L., Beier, E., Avalos-García, C., Lavín, M.F., 2006. Larval fish assemblages and geostrophic circulation in Bahía de La Paz and the surrounding southwestern region of the Gulf of California. J. Plankton Res. 28, 1081–1098.

Santamaría-del-Angel, E., Alvares-Borrego, S., Müller-Karger, F.E., 1994. Gulf of California biogeographic regions based on coastal zone color scanner imagery. J. Geophys. Res. 99 (C4), 7411–7421.

Seibel, B.A., 2011. Critical oxygen levels and metabolic suppression in oxygen minimum zones. J. Exp. Biol 214, 326–336.

Sidón-Ceseña, K. 2012. Variación vertical y estacional de los cocolitofores en la Cuenca Alfonso, Bahía de La Paz (Feb-2007–Ene-2008). Tesis Licenciatura. Universidad Autónoma de Baja California Sur.

Silver, M.W., Gowing, M.M., 1991. The "particle" flux: origins and biological components. Progr. Oceanogr 26, 75–113.

Silverberg, N., Shumilin, E., Aguirre Bahena, F., Rodríguez Castañeda, A.P., Sapozhnikov, D., 2007. The impact of hurricanes on sedimenting particulate matter in the semiarid Bahía de La Paz, Gulf of California. Cont. Shelf Res. 27, 2513–2522.

Silverberg, N., Martínez, A., Aguíñiga, S., Carriquiry, J.D., Romero, N., Choumiline, E., Cota, S., 2004. Contrasts in sedimentation flux below the southern California Current between late 1996 and during the El Niño event of 1997–98. Estuar. Coast. Shelf Sci. 59, 575–587.

Silverberg, N., Sundby, B., Mucci, A., Zhong, S., Arakaki, T., Hall, P., Tenberg, A., Hillemeyer, A., 2000. Carbon mineralization and burial in sediments of the eastern Canadian continental margin. Deep Sea Res. II 47, 699–732.

Signoret, M., Santoyo, H., 1980. Aspectos Ecológicos del Plancton de La Bahía de la Paz Baja California Sur. An. Centro Cienc. Mar Limnol. Univ. Nal. Autón. México 7 (2), 217–248.

Stukel, M.R., Landry, M.R., Benitez-Nelson, C.R., Goerickea, R., 2011. Trophic cycling and carbon export relationships in the California Current Ecosystem. Limnol. Oceanogr. 56, 1866–1878.

Ternon, E., Guieu, C., Loye-Pilot, M.-D., Leblond, N., Bosc, E., Gasser, B., Miquel, J.-C., Martín, J., 2010. The Impact of Saharan Dust on the Particulate Export in the Water Column of the North Western Mediterranean Sea.

Thunell, R., 1997. Continental margin particle flux: seasonal cycles and archives of global change. Oceanus 40, 20–23.

Thunell, R., 1998. Seasonal and annual variability in particle fluxes in the Gulf of California: a response to climate forcing. Deep Sea Res. Part I 45, 2059–2083.

Thunell, R., Benitez-Nelson, C., Varela, R., Astor, Y., Muller-Karger, F., 2007. Particulate organic carbon fluxes along upwelling-dominated continental margins: rates and mechanisms. Global Biogeochem. Cycles 21, GB1022 (htt).

Trull, T.W., Bray, S.G., Buesseler, K.O., Lamborg, C.H., Manganini, S., Moy, C., Valdes, J., 2008. In-situ measurement of mesopelagic particle sinking rates and the control of carbon transfer to the ocean interior during the Vertical Flux in the Global Ocean (VERTIGO) voyages in the North Pacific. Deep Sea Res. Part II 55, 1684–1695.

Urcádiz-Cázares, F.J., 2005. Flujos de cocolitos (cocolitóforos) y su aporte de $CaCO_3$ evaluado con trampa de sedimentos en la Alfonso Basin (Bahía de La Paz), Golfo de California, México. Tesis de Licenciatura. Departamento de Geología. Universidad Autónoma de Baja California Sur. 62 pp.

Verdugo-Díaz, G., Albáñez-Lucero, M.O., Cervantes-Duarte, R., 2008. Estimación de la productividad primaria durante ontoño-invierno en la Bahía de La Paz, B.C.S., México. Oceánides 23 (1–2), 45–53.

Villegas-Aguilera, M.M., 2009. Comparación del fitoplancton siliceo de la zona eufótica y en sedimentación, como señal de la productividad primaria en la Cuenca Alfonso, Golfo de California. M.Sc. Thesis. Centro Interdisciplinario de Ciencias Marinas-IPN. 80p.

Zaytzev, O., Rabinovich, A.B., Thomson, R., Silverberg, N., 2009. Intense diurnal surface currents in the Bay of La Paz, Mexico. Cont. Shelf Res 30, 608–619.